unesp

UNIVERSIDADE ESTADUAL PAULISTA

PROGRAMA DE PÓS-GRADUAÇÃO EM FÍSICA

ÁREA DE CONCENTRAÇÃO EM FÍSICA APLICADA

INSTITUTO DE GEOCIÊNCIAS E CIÊNCIAS EXATAS

RIO CLARO

UNIVERSIDADE ESTADUAL PAULISTA "JÚLIO DE MESQUITA FILHO"
INSTITUTO DE GEOCÊNCIAS E CIÊNCIAS EXATAS
CÂMPUS DE RIO CLARO

Geovane Módena Pereira

Criptografia de Qubits de Férmions de Majorana por meio de Estados Ligados no Contínuo

Dissertação de mestrado apresentada ao Instituto de Geociências e Ciências Exatas da Universidade Estadual Paulista Júlio de Mesquita Filho - UNESP, Câmpus de Rio Claro, como parte dos requisitos para obtenção do título de Mestre em Física, sob a orientação do Prof. Dr. Antonio Carlos Ferreira Seridonio.

RIO CLARO – SP

2018

Geovane Módena Pereira

Criptografia de Qubits de Férmions de Majorana por meio de Estados Ligados no Contínuo

Dissertação de mestrado apresentada ao Instituto de Geocências e Ciências Exatas da Universidade Estadual Paulista Júlio de Mesquita Filho - UNESP, Câmpus de Rio Claro, como parte dos requisitos para obtenção do título de Mestre em Física, sob a orientação do Prof. Dr. Antonio Carlos Ferreira Seridonio.

Comissão Examinadora

Prof. Dr. Antonio Carlos Ferreira Seridonio – UNESP – Ilha Solteira

Prof. Dr. Ricardo Egydio de Carvalho – UNESP – Rio Claro

Prof. Dr. Rafael Zadorosny – UNESP – Ilha Solteira

RIO CLARO – SP

2018

DEFESA DE DISSERTAÇÃO DE MESTRADO DO PROGRAMA DE PÓS-GRADUAÇÃO EM FÍSICA

DISCENTE: GEOVANE MODENA PEREIRA

TÍTULO: Criptografia de Qubits de Férmions de Majorana por meio de Estados Ligados no Contínuo

Data: 01 de Dezembro de 2017 às 14:00

Local: Sala de Videoconferência do Bloco Didático G II

APROVADO (X)   REPROVADO (   )

 PARECER CIRCUNSTANCIADO:

_____

_____

_____

_____

_____

_____

_____

Rio Claro, 01 de Dezembro de 2017

Prof. Dr. Antonio Carlos Ferreira Seridonio

Prof. Dr. Ricardo Egydio de Carvalho

Prof. Dr. Rafael Zadorosny

Resumo

Nós investigamos teoricamente uma cadeia topológica de Kitaev conectada a dois pontos quânticos (QDs) hibridizados a terminais metálicos. Neste sistema, observamos o surgimento de dois fenômenos marcantes: (i) uma decriptografia do Férmion de Majorana (MF), que é detectado por meio de medições de condutância devido ao estado de vazamento assimétrico do qubit de MFs nos QDs; (ii) criptografia desse qubit em ambos os QDs quando o vazamento é simétrico. Em tal regime, temos portanto a criptografia proposta, uma vez que o qubit de MFs separa-se nos QDs como estados ligados no contínuo (BICs), os quais não são detectáveis em experimentos de condutância.

Palavras-chave: Criptografia, MF(Férmion de Majorana), BIC(Estados ligados no contínuo), QD (Ponto quântico), Qubit.

Abstract

We theoretically investigate a topological Kitaev chain connected to a double quantum-dot (QD) setup hybridized with metallic leads. In this system, we observe the emergence of two striking phenomena: i) a decrypted Majorana Fermion (MF) - qubit recorded over a single QD, which is detectable by means of conductance measurements due to the asymmetrical MF-leaked state into the QDs; ii) an encrypted qubit recorded in both QDs when the leakage is symmetrical. In such a regime, we have a cryptography-like manifestation, since the MF-qubit becomes bound states in the continuum, which is not detectable in conductance experiments.

Keywords: Cryptography, MF(Majorana Fermion), BIC(Bound states in the continuum), QD(Quantum dot), Qubit.

Sumário

Lista de Figuras

Capítulo 1

Introdução

Férmions de Majorana (MFs) são partículas de modo zero de energia correspondentes às suas próprias antipartículas [1, 2] e podem aparecer como quasipartículas nas bordas de uma cadeia topológica de Kitaev [3, 4, 5, 6, 7]. Curiosamente, aproximando-se a cadeia de Kitaev a um ponto quântico (QD, Quantum Dot do Inglês), o *qubit* (quantum bit) de um MF no estado vazado [8] manifesta-se como um pico de voltagem zero (ZBP, zero-bias peak em Inglês) em medidas de condutância. O ZBP é a marca de um MF que revela experimentalmente o *qubit* registrado no QD. De fato, tal fenômeno foi confirmado experimentalmente em um QD de nanofio-híbrido feito de InAs/Al [9] com forte interação spin-órbita e campo magnético externo, sendo o nanofio colocado perto de um supercondutor do tipo "s-wave".

Vale ressaltar que os *qubits* de MFs também podem surgir no efeito Hall quântico fracionário com fator de preenchimento $\nu = 5/2$ [10], em isolantes topológicos tridimensionais [11], no núcleo de vórtices super-condutores [12, 13, 14] e nas bordas das cadeias atômicas ferromagnéticas que cobrem supercondutores com uma pronunciada interação spin-órbita [15, 16], de forma semelhante aos nanofios semicondutores [17]. Em termos de aplicações tecnológicas, os MFs são de particular interesse, devido à sua proteção topológica contra o fenômeno de decoerência [3], uma característica chave para a realização de computa-dores quânticos eficientes.

Neste trabalho, mostramos que o emprego de dois QDs, conforme descritos na Fig.1.1 (a), permite a criptografia do *qubit* $\eta_\uparrow = \frac{1}{\sqrt{2}} (\Psi_1 + i\Psi_2)$ composto pelos MFs Ψ_1 e Ψ_2. Nossos principais achados teóricos dependem da interação entre o efeito de vazamento do estado de MF da cadeia de Kitaev e os chamados estados ligados no contínuo (BICs, bound states in the continuum do Inglês) [18, 19]. Nesse contexto, vale a pena recordar a Física subjacente de tais excitações exóticas: os BICs foram propostos por von Neumann e Wigner em 1929 [18] como estados quânticos com funções de onda quadrado integráveis, mas surpreendentemente dentro da região do domínio contínuo de energia. Os BICs constituem um tópico atual de interesse geral [20], aparecendo em vários sistemas físicos como o grafeno [21, 22, 23], a óptica e a fotônica [24, 25, 26, 27], os arranjos que apresentam chiralidade peculiar [28] e estados de Floquet-Hubbard devido a campos alternados [29, 30]. Além disso e como possíveis aplicações, os BICs assistidos por MFs permitem o estocamento de *qubits* [31] e a realização de um seletor de corrente elétrica em
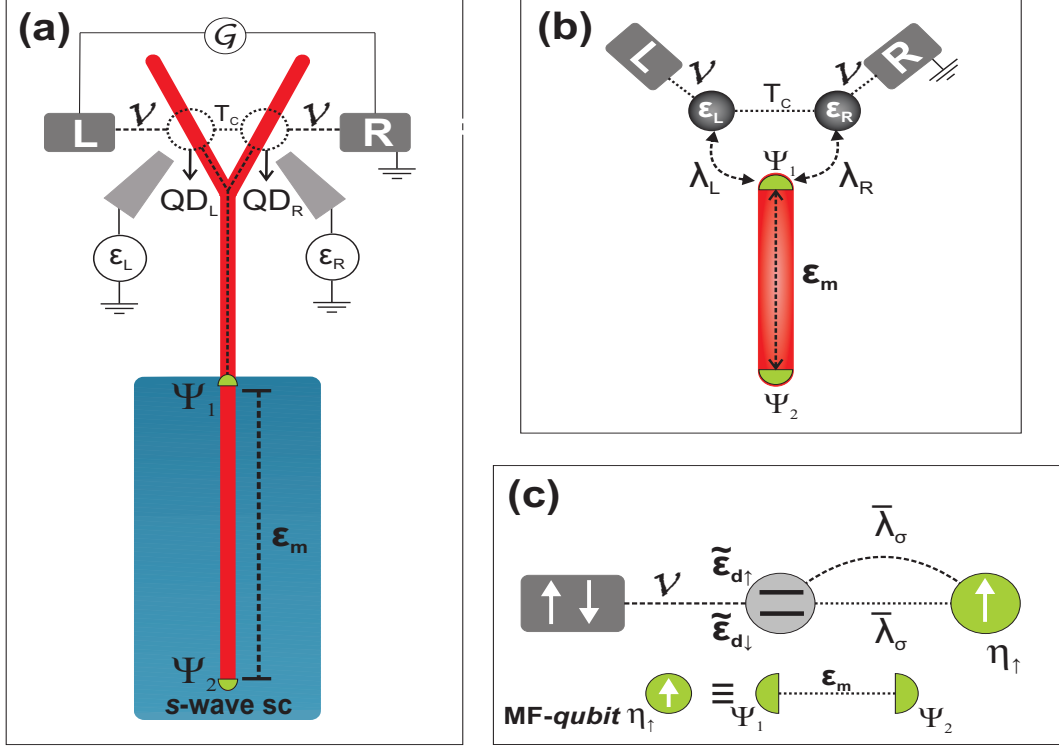
Figura 1.1: (a) Dois QDs simetricamente acoplados aos terminais via hibridização $\mathcal{V}$ e assimetricamente a uma cadeia topológica de Kitaev por meio das amplitudes complexas λ_L e λ_R. Ψ_1 e Ψ_2 são MFs com desdobramento de energia $\varepsilon_M \to 0$. (b) Esboço simplificado do painel (a). (c) Mapeamento do sistema original do painel (b) na representação do *pseudospin*. O hiato *pseudo*-Zeeman renormalizado $\tilde{\epsilon}_{d\uparrow} - \tilde{\epsilon}_{d\downarrow}$ aparece retratado dentro do QD central, lateralmente acoplado ao *qubit* $\eta_\uparrow$. $\bar{\lambda}_\sigma$ identifica o tunelamento e a energia de ligação do par Cooper entre o QD e $\eta_\uparrow$, respectivamente dados pelas linhas tracejadas horizontais e semi-circulares.

nanoescala [32].

Devemos mencionar que os elétrons armadilhados nos BICs são impedidos de decaírem no contínuo de energia do meio. Consequentemente, chamamos de criptografia do *qubit* $\eta_\uparrow = \frac{1}{\sqrt{2}}\left(\Psi_1 + i\Psi_2\right)$ quando sua assinatura ZBP desaparece como um BIC, tornando-se indetectável por medições de condutância. Como será discutido nesta dissertação, também descobrimos um vazamento assimétrico desse *qubit*. Nessa situação, o ZBP é visível na condutância e chamamos esse regime por *qubit* decriptado. Tal caso corresponde à leitura do *qubit* em QDs caracterizado por um ZBP, conforme proposto por Flensberg [33]. Caso contrário, a criptografia do *qubit* é obtida quando o vazamento é simétrico sobre os QDs, mas com um ZBP invisível na condutância. Nesse regime, o estado vazado do *qubit* de MFs é dividido nos dois QDs como BICs.

Capítulo 2

Supercondutividade topológica

Começamos com a revisão do modelo de Kitaev, para um supercondutor 1D do tipo "p" e com elétrons sem spin [1]. Neste modelo, os férmions de Majorana (modo zero de energia) aparecem em uma forma muito simples. Seguindo Kitaev, introduzimos o Hamiltoniano:

$$H = -\mu \sum_x c_x^\dagger c_x - \frac{1}{2} \sum_x \left(t c_x^\dagger c_{x+1} + \triangle e^{i\phi} c_x c_{x+1} + \text{H.c.} \right), \tag{2.1}$$

onde μ é o potencial químico, t é o acoplamento entre vizinhos mais próximos, $\triangle$ é a amplitude de pareamento do tipo"p" e ϕ é a fase supercondutora correspondente. Por simplicidade, ajustamos a constante de rede à unidade.

Os operadores fermiônicos c_x do Hamiltoniano original da Eq. (2.1) podem ser decompostos em termos de dois férmions de Majorana, utilizando-se a seguinte transformação:

$$c_x = \frac{e^{-i\phi/2}}{2} \left(\gamma_{B,x} + i\gamma_{A,x} \right) \tag{2.2}$$

e

$$c_x^\dagger = \frac{e^{i\phi/2}}{2} \left(\gamma_{B,x} - i\gamma_{A,x} \right), \tag{2.3}$$

onde os operadores do lado direito obedecem às relações canônicas dos férmions de Majorana

$$\gamma_{\alpha,x} = \gamma_{\alpha,x}^\dagger \tag{2.4}$$

e

$$\{\gamma_{\alpha,x}, \gamma_{\alpha',x'}\} = 2\delta_{\alpha\alpha'}\delta_{xx'}. \tag{2.5}$$

Da Eq. (2.5), temos que

$$\gamma_{\alpha,x}\gamma_{\alpha,x} + \gamma_{\alpha,x}\gamma_{\alpha,x} = 2$$

$$2\gamma_{\alpha,x}\gamma_{\alpha,x} = 2$$

$$\gamma_{\alpha,x}^2 = 1. \tag{2.6}$$

Substituindo os operadores c_x e $c_x^\dagger$ no Hamiltoniano da Eq. (2.1), temos:

$$
\begin{aligned}
H = &-\mu \sum_x \frac{e^{i\phi/2}}{2}\left(\gamma_{B,x} - i\gamma_{A,x}\right)\frac{e^{-i\phi/2}}{2}\left(\gamma_{B,x} + i\gamma_{A,x}\right) \\
&- \frac{1}{2}\sum_x t\frac{e^{i\phi/2}}{2}\left(\gamma_{B,x} - i\gamma_{A,x}\right)\frac{e^{-i\phi/2}}{2}\left(\gamma_{B,x+1} + i\gamma_{A,x+1}\right) \\
&- \frac{1}{2}\sum_x \Delta e^{i\phi}\frac{e^{-i\phi/2}}{2}\left(\gamma_{B,x} + i\gamma_{A,x}\right)\frac{e^{-i\phi/2}}{2}\left(\gamma_{B,x+1} + i\gamma_{A,x+1}\right) \\
&- \frac{1}{2}\sum_x -t\frac{e^{-i\phi/2}}{2}\left(\gamma_{B,x} + i\gamma_{A,x}\right)\frac{e^{i\phi/2}}{2}\left(\gamma_{B,x+1} - i\gamma_{A,x+1}\right) \\
&+ \frac{1}{2}\sum_x \Delta e^{-i\phi}\frac{e^{i\phi/2}}{2}\left(\gamma_{B,x} - i\gamma_{A,x}\right)\frac{e^{i\phi/2}}{2}\left(\gamma_{B,x+1} - i\gamma_{A,x+1}\right).
\end{aligned}
\tag{2.7}
$$

Simplificando,

$$
\begin{aligned}
H = &-\frac{\mu}{4}\sum_x \left(\gamma_{B,x}\gamma_{B,x} + i\gamma_{B,x}\gamma_{A,x} - i\gamma_{A,x}\gamma_{B,x} + \gamma_{A,x}\gamma_{A,x}\right) \\
&- \frac{1}{2}\sum_x \frac{t}{4}\left(\gamma_{B,x}\gamma_{B,x+1} + i\gamma_{B,x}\gamma_{A,x+1} - i\gamma_{A,x}\gamma_{B,x+1} + \gamma_{A,x}\gamma_{A,x+1}\right) \\
&- \frac{1}{2}\sum_x \frac{\Delta}{4}\left(\gamma_{B,x}\gamma_{B,x+1} + i\gamma_{B,x}\gamma_{A,x+1} + i\gamma_{A,x}\gamma_{B,x+1} - \gamma_{A,x}\gamma_{A,x+1}\right) \\
&+ \frac{1}{2}\sum_x \frac{t}{4}\left(\gamma_{B,x}\gamma_{B,x+1} - i\gamma_{B,x}\gamma_{A,x+1} + i\gamma_{A,x}\gamma_{B,x+1} + \gamma_{A,x}\gamma_{A,x+1}\right) \\
&+ \frac{1}{2}\sum_x \frac{\Delta}{4}\left(\gamma_{B,x}\gamma_{B,x+1} - i\gamma_{B,x}\gamma_{A,x+1} - i\gamma_{A,x}\gamma_{B,x+1} - \gamma_{A,x}\gamma_{A,x+1}\right).
\end{aligned}
\tag{2.8}
$$

Simplificando novamente,

$$
\begin{aligned}
H = &-\frac{\mu}{4}\sum_x \left(\gamma_{B,x}\gamma_{B,x} + \gamma_{A,x}\gamma_{A,x} + i\gamma_{B,x}\gamma_{A,x} - i\gamma_{A,x}\gamma_{B,x}\right) \\
&- \frac{1}{2}\sum_x \frac{t}{4}\left(i\gamma_{B,x}\gamma_{A,x+1} - i\gamma_{A,x}\gamma_{B,x+1} + i\gamma_{B,x}\gamma_{A,x+1} - i\gamma_{A,x}\gamma_{B,x+1}\right) \\
&- \frac{1}{2}\sum_x \frac{\Delta}{4}\left(i\gamma_{B,x}\gamma_{A,x+1} + i\gamma_{A,x}\gamma_{B,x+1} + i\gamma_{B,x}\gamma_{A,x+1} + i\gamma_{A,x}\gamma_{B,x+1}\right).
\end{aligned}
\tag{2.9}
$$
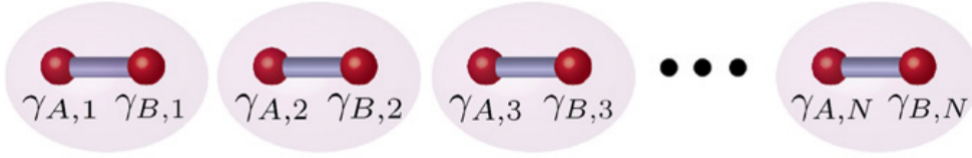
Figura 2.1: Representação esquemática da fase trivial [1]. Os círculos de cor vermelha representam os férmions de Majorana, as barras de cor roxa representam os acoplamentos entre eles e as elipses de cor lilás representam os sítios da rede.

Empregando as relações $\{\gamma_{A,x}, \gamma_{B,x}\} = 0$, $\gamma_{\alpha,x}^2 = 1$,

$$
\begin{aligned}
H = &-\frac{\mu}{4} \sum_{x=1}^{N} \left(1 + 1 + i\gamma_{B,x}\gamma_{A,x} + i\gamma_{B,x}\gamma_{A,x} \right) \\
&- \frac{1}{2} \sum_{x=1}^{N-1} \left[\frac{t}{4} \left(2i\gamma_{B,x}\gamma_{A,x+1} - 2i\gamma_{A,x}\gamma_{B,x+1} \right) \right] \\
&- \frac{1}{2} \sum_{x=1}^{N-1} \left[\frac{\Delta}{4} \left(2i\gamma_{B,x}\gamma_{A,x+1} + 2i\gamma_{A,x}\gamma_{B,x+1} \right) \right].
\end{aligned}
\tag{2.10}
$$

Simplificando, obtemos:

$$
\begin{aligned}
H = &-\frac{\mu}{4} \sum_{x=1}^{N} \left(2 + 2i\gamma_{B,x}\gamma_{A,x} \right) \\
&- \frac{i}{2} \sum_{x=1}^{N-1} \left[\frac{t}{2} \left(\gamma_{B,x}\gamma_{A,x+1} - \gamma_{A,x}\gamma_{B,x+1} \right) \right] \\
&- \frac{i}{2} \sum_{x=1}^{N-1} \left[\frac{\Delta}{2} \left(\gamma_{B,x}\gamma_{A,x+1} + \gamma_{A,x}\gamma_{B,x+1} \right) \right].
\end{aligned}
\tag{2.11}
$$

Por fim, o Hamiltoniano de Kitaev, escrito utilizando a base dos operadores de Majorana, fica:

$$
H = -\frac{\mu}{2} \sum_{x=1}^{N} \left(1 + i\gamma_{B,x}\gamma_{A,x} \right) - \frac{i}{4} \sum_{x=1}^{N-1} \left[(\Delta + t)\gamma_{B,x}\gamma_{A,x+1} + (\Delta - t)\gamma_{A,x}\gamma_{B,x+1} \right].
\tag{2.12}
$$

2.1 Fase trivial

Este caso corresponde a $\mu \neq 0$ e $t = \Delta = 0$ e é chamada de fase trivial. Note que, o segundo termo da Eq. (2.12) se cancela, de modo que, apenas o acoplamento entre os Majoranas $\gamma_{A,x}$ e $\gamma_{B,x}$ do mesmo sítio da rede sobrevive. Assim, o Hamiltoniano torna-se:

$$
H = -\frac{\mu}{2} \sum_{x=1}^{N} \left(1 + i\gamma_{B,x}\gamma_{A,x} \right).
\tag{2.13}
$$

A figura 2.1 é uma representação para este caso.
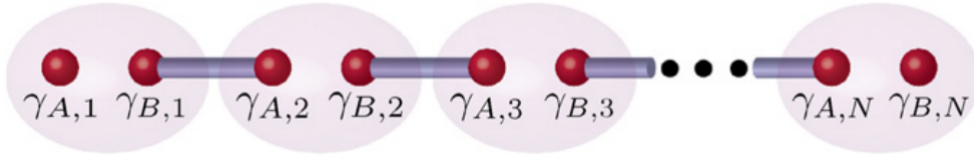
Figura 2.2: Representação esquemática da fase topológica [1]. Os círculos de cor vermelha representam os férmions de Majorana, as barras de cor roxa representam os acoplamentos entre eles e as elipses de cor lilás representam os sítios da rede.

2.2 Fase topológica

O segundo caso é obtido fazendo-se o limite $\mu = 0$ e $t = \Delta \neq 0$, o qual resulta na fase topológica. No Hamiltoniano da Eq. (2.12), o primeiro termo se anula, juntamente com parte do segundo, de modo que:

$$H = -i\frac{t}{2}\sum_{x=1}^{N-1}\gamma_{B,x}\gamma_{A,x+1},\tag{2.14}$$

onde estão acoplados os Majoranas de sítios adjacentes, $\gamma_{B,x}$ e $\gamma_{A,x+1}$. A característica mais marcante aqui é devido aos dois férmions de Majorana isolados nas bordas, ou seja, $\gamma_{A,1}$ e $\gamma_{B,N}$. É devido a esses férmions isolados desacoplados do meio, que a computação quântica vem dando considerável atenção, pois acredita-se na possibilidade de criação de *qubits* imunes à decoerência utilizando-se de tais férmions. A figura 2.2 ilustra tal regime.

Capítulo 3

Hamiltoniano de Anderson e Funções de Green

3.1 Hamiltoniano de Anderson

Aqui daremos uma breve discussão de como o modelo de Anderson [34] emerge, pois é a base do Hamiltoniano desta dissertação. Tradicionalmente, discutimos esse modelo para uma única impureza. Anderson assumiu uma impureza como um estado localizado, de modo que, somente os orbitais mais externos dela hibridizam-se com os elétrons de condução. O modelo também assume que a repulsão de Coulomb é entre elétrons de spins contrários localizados apenas na impureza.
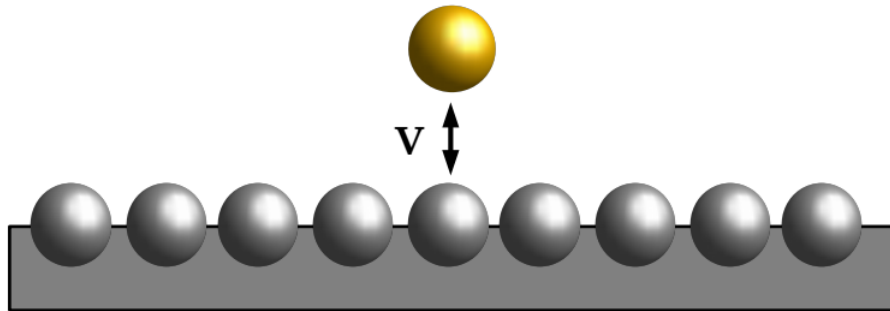
Figura 3.1: (a) Representação esquemática do modelo de Anderson [34]. A hibridização é $\mathcal{V}$ entre a impureza e o hospedeiro.

Agora iremos descrever o modelo de Anderson de uma impureza (*SIAM: Single Impurity Anderson Model*), que é apresentado em segunda quantização. A figura (3.1) sumariza o Hamiltoniano:

$$\mathcal{H}_{SIAM} = \mathcal{H}_{hosp} + \mathcal{H}_{imp} + \mathcal{H}_{hib}. \tag{3.1}$$

O primeiro termo é para a banda de condução do metal dada por um gás de elétrons livres com energia

$\varepsilon_{\mathbf{k}}$ e número de onda $\mathbf{k}$:

$$\mathcal{H}_{hosp} = \sum_{\mathbf{k}\sigma} \varepsilon_{\mathbf{k}} c_{\mathbf{k}\sigma}^{\dagger} c_{\mathbf{k}\sigma}, \tag{3.2}$$

onde $c_{\mathbf{k}\sigma}^{\dagger}(c_{\mathbf{k}\sigma})$ cria (aniquila) um elétron com spin σ e número de onda $\mathbf{k}$. A impureza é um único estado degenerado com energia ε_d que corresponde a um orbital d (ou f). Este estado pode ser ocupado por dois elétrons de spins opostos que se repelem pelo Coulomb U, ou seja,

$$\mathcal{H}_{imp} = \sum_{\sigma} \varepsilon_{d\sigma} d_{\sigma}^{\dagger} d_{\sigma} + U d_{\uparrow}^{\dagger} d_{\uparrow} d_{\downarrow}^{\dagger} d_{\downarrow}. \tag{3.3}$$

O último termo do Hamiltoniano da equação (3.1) compreende a hibridização com amplitude $\mathcal{V}$ dos elétrons itinerantes do hospedeiro com a impureza, isto é,

$$\mathcal{H}_{hib} = \sum_{\mathbf{k}\sigma} \mathcal{V} \left(c_{\mathbf{k}\sigma}^{\dagger} d_{\sigma} + \text{H.c.} \right). \tag{3.4}$$

3.2 Funções de Green

As funções de Green (FGs) são utilizadas como ferramentas matemáticas para resolver equações diferenciais, sendo que aqui serão empregadas para resolver um problema de Mecânica Quântica [35] em segunda quantização. O próposito desta dissertação é portanto, a descrição da propagação dos elétrons em um sistema de Física do Estado Sólido.

As funções de Green retardada e avançada de uma partícula são:

$$\mathcal{G}^{\mathcal{R}}(\mathbf{r}, \tau; \mathbf{r}', \tau') = -\frac{i}{\hbar} \theta(\tau - \tau') \left\langle \left[\Psi(\mathbf{r}, \tau), \Psi^{\dagger}(\mathbf{r}', \tau') \right]_{+} \right\rangle, \tag{3.5}$$

$$\mathcal{G}^{\mathcal{A}}(\mathbf{r}, \tau; \mathbf{r}', \tau') = \frac{i}{\hbar} \theta(\tau' - \tau) \left\langle \left[\Psi(\mathbf{r}, \tau), \Psi^{\dagger}(\mathbf{r}', \tau') \right]_{+} \right\rangle, \tag{3.6}$$

onde $\theta(\tau - \tau')$ é a função degrau, $[...]_{+}$ é o anticomutador e $\langle ... \rangle$ determina uma média termodinâmica, a qual é:

$$\left\langle \left[\Psi(\mathbf{r}', \tau'), \Psi^{\dagger}(\mathbf{r}, \tau) \right]_{+} \right\rangle = \frac{1}{Z} \text{Tr} \left\{ e^{-\beta H} \left[\Psi(\mathbf{r}', \tau'), \Psi^{\dagger}(\mathbf{r}, \tau) \right]_{+} \right\}, \tag{3.7}$$

em que a função partição é $Z = \text{Tr} \left\{ e^{-\beta H} \right\}$, H é o Hamiltoniano, Tr representa o traço e $\beta = \frac{1}{k_B T}$.

Consideremos um estado $|n>$ que é do Hamiltoniano ($H|n> = E_n|n>$), assim:

$$\mathcal{G}^{\mathcal{R}}(\mathbf{r}, \tau; \mathbf{r}', \tau') = -\frac{i}{\hbar} \theta(\tau - \tau') \sum_{n} \frac{1}{Z} e^{-\beta E_n} <n| \left[\Psi(\mathbf{r}, \tau), \Psi^{\dagger}(\mathbf{r}', \tau') \right]_{+} |n>, \tag{3.8}$$

$$\mathcal{G}^{\mathcal{A}}(\mathbf{r}, \tau; \mathbf{r}', \tau') = \frac{i}{\hbar}\theta(\tau' - \tau)\sum_n \frac{1}{Z}e^{-\beta E_n} < n|\left[\Psi(\mathbf{r}, \tau), \Psi^\dagger(\mathbf{r}', \tau')\right]_+ |n >, \tag{3.9}$$

onde

$$\mathcal{G}^{\mathcal{R}}(\mathbf{r}, \tau; \mathbf{r}', \tau') = \left[\mathcal{G}^{\mathcal{A}}(\mathbf{r}, \tau; \mathbf{r}', \tau')\right]^\dagger. \tag{3.10}$$

Como vimos, a função de Green é definida na variável tempo, mas usaremos uma transformada de Fourier do espaço dos tempos para o das energias, pois é nesse último espaço que estudamos o transporte eletrônico. Para tal, usaremos o método da equação do movimento (*EOM: equation of motion*) [35] descrito a seguir. Utilizemos para esse propósito, a definição de uma função de Green retardada com dois operadores fermiônicos $\hat{A}$ e $\hat{B}$ na representação de Heisenberg:

$$\mathcal{G}^{\mathcal{R}}_{\mathcal{AB}}(\tau, 0) = -\frac{i}{\hbar}\theta(\tau - 0)\left\langle \left[\hat{A}(\tau), \hat{B}^\dagger(0)\right]_+ \right\rangle. \tag{3.11}$$

Fazendo Fourier:

$$
\begin{aligned}
\tilde{\mathcal{G}}^{\mathcal{R}}_{\mathcal{AB}}(\varepsilon) &= \frac{i\hbar}{(\varepsilon + i\eta)}\int_{-\infty}^{\infty} d\tau \frac{\partial}{\partial\tau}\left\{-\frac{i}{\hbar}\theta(\tau - 0)\left\langle\left[\hat{A}(\tau), \hat{B}^\dagger(0)\right]_+\right\rangle\right\}e^{\frac{i}{\hbar}(\varepsilon + i\eta)\tau} \\
&= \frac{1}{(\varepsilon + i\eta)}\int_{-\infty}^{\infty} d\tau \frac{\partial}{\partial\tau}\left\{\theta(\tau - 0)\left\langle\left[\hat{A}(\tau), \hat{B}^\dagger(0)\right]_+\right\rangle\right\}e^{\frac{i}{\hbar}(\varepsilon + i\eta)\tau},
\end{aligned}
\tag{3.12}
$$

onde o infinitesimal é $\eta \to 0^+$. Efetuando a derivada temporal,

$$
\begin{aligned}
\tilde{\mathcal{G}}^{\mathcal{R}}_{\mathcal{AB}}(\varepsilon) &= \frac{1}{(\varepsilon + i\eta)}\int_{-\infty}^{\infty} d\tau \frac{\partial}{\partial\tau}\theta(\tau - 0)\left\{\left\langle\left[\hat{A}(\tau), \hat{B}^\dagger(0)\right]_+\right\rangle\right\}e^{\frac{i}{\hbar}(\varepsilon + i\eta)\tau} \\
&+ \int_{-\infty}^{\infty} d\tau \left\{\theta(\tau - 0)\left\langle\left[\frac{\partial}{\partial\tau}\hat{A}(\tau), \hat{B}^\dagger(0)\right]_+\right\rangle\right\}e^{\frac{i}{\hbar}(\varepsilon + i\eta)\tau}.
\end{aligned}
\tag{3.13}
$$

Desse modo,

$$
\begin{aligned}
\tilde{\mathcal{G}}^{\mathcal{R}}_{\mathcal{AB}}(\varepsilon) &= \frac{1}{(\varepsilon + i\eta)}\int_{-\infty}^{\infty} d\tau \delta(\tau - 0)\left\{\left\langle\left[\hat{A}(\tau), \hat{B}^\dagger(0)\right]_+\right\rangle\right\}e^{\frac{i}{\hbar}(\varepsilon + i\eta)\tau} \\
&+ \frac{1}{(\varepsilon + i\eta)}\int_{-\infty}^{\infty} d\tau \left\{\theta(\tau - 0)\left\langle\left[\frac{i}{\hbar}\left[H, \hat{A}\right], \hat{B}^\dagger(0)\right]_+\right\rangle\right\}e^{\frac{i}{\hbar}(\varepsilon + i\eta)\tau},
\end{aligned}
\tag{3.14}
$$

resolvendo o primeiro termo, encontramos:

$$
\begin{aligned}
\tilde{\mathcal{G}}^{\mathcal{R}}_{\mathcal{AB}}(\varepsilon) &= \frac{1}{(\varepsilon + i\eta)}\left\langle\left[\hat{A}(0), \hat{B}^\dagger(0)\right]_+\right\rangle \\
&+ \frac{1}{(\varepsilon + i\eta)}\int_{-\infty}^{\infty} d\tau \left\{-\frac{i}{\hbar}\theta(\tau - 0)\left\langle\left[\frac{i}{\hbar}\left[H, \hat{A}\right], \hat{B}^\dagger(0)\right]_+\right\rangle\right\}e^{\frac{i}{\hbar}(\varepsilon + i\eta)\tau}
\end{aligned}
\tag{3.15}
$$

e reconhecendo a função de Green $\tilde{\mathcal{G}}^{\mathcal{R}}_{[\mathcal{H},\mathcal{A}]\mathcal{B}}(\varepsilon)$, obtemos:

$$(\varepsilon + i\eta)\tilde{\mathcal{G}}^{\mathcal{R}}_{\mathcal{AB}}(\varepsilon) = \left\langle\left[\hat{A}, \hat{B}^\dagger\right]_+\right\rangle + \tilde{\mathcal{G}}^{\mathcal{R}}_{[\mathcal{H},\mathcal{A}]\mathcal{B}}(\varepsilon). \tag{3.16}$$

Capítulo 4

Quantum Dots (QDs) em paralelo

4.1 Sistema de dois QDs

Embora esta disertação seja para dois QDs em série, mas para fins didáticos, vamos considerar inicialmente o caso de dois QDs em paralelo e em seguida, particularizar para um único QD. Aqui temos o intuito de reproduzir o resultado principal da Ref.[36], ou seja, a FG de um QD acoplado a terminais metálicos e um fio de Kitaev na fase topológica. O Hamiltoniano é:

$$
\begin{aligned}
\mathcal{H}_e &= \sum_k \varepsilon_k c_{ek}^\dagger c_{ek} + \sum_{jk} \sqrt{\frac{2}{\mathcal{N}}} V \left(c_{ek}^\dagger d_j + H.c. \right) + \sum_j \varepsilon_j d_j^\dagger d_j + \sum_{kq} \frac{V_{BT}}{\mathcal{N}} c_{ek}^\dagger c_{eq} \\
&+ i\epsilon_M \eta_1 \eta_2 + \lambda \left(d_1 - d_1^\dagger \right) \eta_1,
\end{aligned}
\tag{4.1}
$$

Nesta subseção nós determinamos as FGs $\tilde{\mathcal{G}}_{d_j d_j}(\varepsilon)$ e $\tilde{\mathcal{G}}_{d_j d_{\bar{j}}}(\varepsilon)$. Vamos começar introduzindo a representação dos Majoranas

$$
\eta_1 = \frac{1}{\sqrt{2}} \left(f^\dagger + f \right)
\tag{4.2}
$$

e

$$
\eta_2 = i \frac{1}{\sqrt{2}} \left(f^\dagger - f \right).
\tag{4.3}
$$

Assim temos:

$$
\begin{aligned}
i\epsilon_M \eta_1 \eta_2 &= -\epsilon_M \frac{1}{2} \left(f^\dagger f^\dagger - f^\dagger f + f f^\dagger - f f \right) \\
&= -\epsilon_M \frac{1}{2} \left(-f^\dagger f + f f^\dagger \right) \\
&= -\epsilon_M \frac{1}{2} \left(-f^\dagger f + 1 - f^\dagger f \right) \\
&= \epsilon_M \left(f^\dagger f - \frac{1}{2} \right),
\end{aligned}
\tag{4.4}
$$

$$\lambda \left(d_1 - d_1^\dagger \right) \eta_1 = \frac{\lambda}{\sqrt{2}} \left(d_1 - d_1^\dagger \right) \left(f^\dagger + f \right)$$

$$= \frac{\lambda}{\sqrt{2}} \left(d_1 f^\dagger + d_1 f - d_1^\dagger f^\dagger - d_1^\dagger f \right) \tag{4.5}$$

e

$$\begin{aligned}
\mathcal{H}_e &= \sum_k \varepsilon_k c_{ek}^\dagger c_{ek} + \sum_{jk} \sqrt{\frac{2}{\mathcal{N}}} V \left(c_{ek}^\dagger d_j + H.c. \right) + \sum_j \varepsilon_j d_j^\dagger d_j + \sum_{kq} \frac{V_{BT}}{\mathcal{N}} c_{ek}^\dagger c_{eq} \\
&+ \epsilon_M \left(f^\dagger f - \frac{1}{2} \right) + \frac{\lambda}{\sqrt{2}} \left(d_1 f^\dagger + d_1 f - d_1^\dagger f^\dagger - d_1^\dagger f \right).
\end{aligned} \tag{4.6}$$

Agora nós consideramos a FG

$$\mathcal{G}_{d_j d_j}(t) = -\frac{i}{\hbar} \theta(t) \mathcal{Z}_e^{-1} \sum_n e^{-\beta E_n} \langle n | \left[d_j(t), d_j^\dagger(0) \right]_+ | n \rangle \tag{4.7}$$

e

$$\begin{aligned}
\frac{\partial}{\partial t} \mathcal{G}_{d_j d_j}(t) &= -\frac{i}{\hbar} \delta(t) \mathcal{Z}_e^{-1} \sum_n e^{-\beta E_n} \langle n | \left[d_j(t), d_j^\dagger(0) \right]_+ | n \rangle \\
&+ \left(-\frac{i}{\hbar} \right) \theta(t) \mathcal{Z}_e^{-1} \sum_n e^{-\beta E_n} \langle n | \left[\frac{\partial}{\partial t} d_j(t), d_j^\dagger(0) \right]_+ | n \rangle.
\end{aligned} \tag{4.8}$$

Agora substituimos a relação

$$\begin{aligned}
\frac{\partial}{\partial t} d_j(t) &= -\frac{i}{\hbar} [d_j, \mathcal{H}_e] = -\frac{i}{\hbar} \left\{ \varepsilon_j d_j(t) + \sqrt{\frac{2}{\mathcal{N}}} V \sum_k c_k(t) \right\} \\
&+ \left(-\frac{i}{\hbar} \right) (-\delta_{j1}) \lambda \eta_1(t)
\end{aligned} \tag{4.9}$$

na Eq. (4.8), onde consideramos

$$\begin{aligned}
\left[d_j, \frac{\lambda}{\sqrt{2}} \left(d_1 f^\dagger + d_1 f - d_1^\dagger f^\dagger - d_1^\dagger f \right) \right] &= \frac{\lambda}{\sqrt{2}} \left[d_j, \left(d_1 f^\dagger + d_1 f - d_1^\dagger f^\dagger - d_1^\dagger f \right) \right] \\
&= \frac{\lambda}{\sqrt{2}} \left(d_j d_1 f^\dagger + d_j d_1 f - d_j d_1^\dagger f^\dagger - d_j d_1^\dagger f \right) \\
&- \frac{\lambda}{\sqrt{2}} \left(d_1 f^\dagger d_j + d_1 f d_j - d_1^\dagger f^\dagger d_j - d_1^\dagger f d_j \right)
\end{aligned}$$

$$d_j d_1 f^\dagger + d_j d_1 f - d_j d_1^\dagger f^\dagger - d_j d_1^\dagger f - d_1 f^\dagger d_j - d_1 f d_j + d_1^\dagger f^\dagger d_j + d_1^\dagger f d_j$$

$$= -d_j d_1^\dagger f^\dagger - d_j d_1^\dagger f + d_1^\dagger f^\dagger d_j + d_1^\dagger f d_j$$

$$= -d_j d_1^\dagger f^\dagger + d_1^\dagger f^\dagger d_j - d_j d_1^\dagger f + d_1^\dagger f d_j$$

$$= -d_j d_1^\dagger f^\dagger - d_1^\dagger d_j f^\dagger - d_j d_1^\dagger f - d_1^\dagger d_j f$$

$$= -\left(d_j d_1^\dagger + d_1^\dagger d_j\right) f - \left(d_j d_1^\dagger + d_1^\dagger d_j\right) f^\dagger$$

$$= -\delta_{j1}\left(f^\dagger + f\right), \tag{4.10}$$

$$\left[d_j, \sum_{\tilde{j}k}\sqrt{\frac{2}{\mathcal{N}}}V c_k^\dagger d_{\tilde{j}}\right] \quad + \quad \left[d_{j\sigma}, \sum_{\tilde{j}k}\sqrt{\frac{2}{\mathcal{N}}}V d_{\tilde{j}}^\dagger c_k\right]$$

$$= \sum_{\tilde{j}k}\sqrt{\frac{2}{\mathcal{N}}}V \quad \times \quad \left(d_j c_k^\dagger d_{\tilde{j}} - c_k^\dagger d_{\tilde{j}} d_j\right)$$

$$+ \sum_{\tilde{j}k}\sqrt{\frac{2}{\mathcal{N}}}V \quad \times \quad \left(d_j d_{\tilde{j}}^\dagger c_k - d_{\tilde{j}}^\dagger c_k d_j\right)$$

$$= \sum_{\tilde{j}k}\sqrt{\frac{2}{\mathcal{N}}}V \quad \times \quad \left(c_k^\dagger d_{\tilde{j}} d_j - c_k^\dagger d_{\tilde{j}} d_j\right)$$

$$+ \sum_{\tilde{j}k}\sqrt{\frac{2}{\mathcal{N}}}V \quad \times \quad \left(\delta_{j\tilde{j}} c_k - d_{\tilde{j}}^\dagger d_{j\sigma} c_k - d_{\tilde{j}}^\dagger c_k d_j\right)$$

$$= \sum_{\tilde{j}k}\sqrt{\frac{2}{\mathcal{N}}}V \quad \times \quad \left(\delta_{j\tilde{j}} c_k - d_{\tilde{j}}^\dagger d_j c_k + d_{\tilde{j}}^\dagger d_j c_k\right)$$

$$= \sum_k \sqrt{\frac{2}{\mathcal{N}}}V c_k \tag{4.11}$$

e

$$\left[d_j, \sum_{\tilde{j}}\varepsilon_{\tilde{j}} d_{\tilde{j}}^\dagger d_{\tilde{j}}\right] \quad = \quad \sum_{\tilde{j}}\varepsilon_{\tilde{j}}\left[d_j, d_{\tilde{j}}^\dagger d_{\tilde{j}}\right]$$

$$= \quad \sum_{\tilde{j}}\varepsilon_{\tilde{j}}\left(d_j d_{\tilde{j}}^\dagger d_{\tilde{j}} - d_{\tilde{j}}^\dagger d_{\tilde{j}} d_j\right)$$

$$= \quad \sum_{\tilde{j}}\varepsilon_{\tilde{j}}\left(\delta_{j\tilde{j}} d_{\tilde{j}} - d_{\tilde{j}}^\dagger d_j d_{\tilde{j}} - d_{\tilde{j}}^\dagger d_{\tilde{j}} d_j\right)$$

$$= \quad \sum_{\tilde{j}}\varepsilon_{\tilde{j}}\left(\delta_{j\tilde{j}} d_{\tilde{j}} - d_{\tilde{j}}^\dagger d_j d_{\tilde{j}} - d_{\tilde{j}}^\dagger d_{\tilde{j}} d_j\right)$$

$$= \quad \sum_{\tilde{j}}\varepsilon_{\tilde{j}}\left(\delta_{j\tilde{j}} d_{\tilde{j}} + d_{\tilde{j}}^\dagger d_{\tilde{j}} d_j - d_{\tilde{j}}^\dagger d_{\tilde{j}} d_j\right)$$

$$= \quad \varepsilon_j d_j, \tag{4.12}$$

de modo que,

$$\frac{\partial}{\partial t}\mathcal{G}_{d_j d_j}(t) = \left(-\frac{i}{\hbar}\right)\delta(t)\,\mathcal{Z}_e^{-1}\sum_n e^{-\beta E_n}\,\langle n|\left[d_j(t),d_j^\dagger(0)\right]_+|n\rangle$$

$$+\left(-\frac{i}{\hbar}\right)\varepsilon_j\left\{-\frac{i}{\hbar}\theta(t)\,\mathcal{Z}_e^{-1}\sum_n e^{-\beta E_n}\,\langle n|\left[d_j(t),d_j^\dagger(0)\right]_+|n\rangle\right\}$$

$$+\left(-\frac{i}{\hbar}\right)\sqrt{2}V\left\{-\frac{i}{\hbar}\theta(t)\,\mathcal{Z}_e^{-1}\sum_n e^{-\beta E_n}\,\langle n|\left[\frac{1}{\sqrt{\mathcal{N}}}\sum_k c_k(t),d_j^\dagger(0)\right]_+|n\rangle\right\}$$

$$+\left(-\frac{i}{\hbar}\right)(-\delta_{j1})\lambda\left\{-\frac{i}{\hbar}\theta(t)\,\mathcal{Z}_e^{-1}\sum_n e^{-\beta E_n}\,\langle n|\left[\eta_1(t),d_j^\dagger(0)\right]_+|n\rangle\right\}. \tag{4.13}$$

Levando em conta

$$\mathcal{G}_{\eta_1,d_j}(t) = -\frac{i}{\hbar}\theta(t)\,\mathcal{Z}_e^{-1}\sum_n e^{-\beta E_n}\,\langle n|\left[\eta_1(t),d_j^\dagger(0)\right]_+|n\rangle \tag{4.14}$$

na Eq. (4.13), encontramos

$$\frac{\partial}{\partial t}\mathcal{G}_{d_j d_j}(t) = \left(-\frac{i}{\hbar}\right)\delta(t)\,\mathcal{Z}_e^{-1}\sum_n e^{-\beta E_n}\,\langle n|\left[d_j(t),d_j^\dagger(0)\right]_+|n\rangle - \frac{i}{\hbar}\varepsilon_j\mathcal{G}_{d_j d_j}(t)$$

$$+\left(-\frac{i}{\hbar}\right)\sqrt{2}V\mathcal{G}_{f_e d_j}(t) - \frac{i}{\hbar}(-\delta_{j1})\lambda\mathcal{G}_{\eta_1,d_j}(t). \tag{4.15}$$

Em coordenadas de energia, a Eq. (4.15) torna-se

$$(\varepsilon + i\eta)\,\tilde{\mathcal{G}}_{d_j d_j}(\varepsilon) \quad = \quad 1 + \varepsilon_j\tilde{\mathcal{G}}_{d_j d_j}(\varepsilon) + \sqrt{2}V\tilde{\mathcal{G}}_{f_e d_j}(\varepsilon) - \delta_{j1}\lambda\tilde{\mathcal{G}}_{\eta_1,d_j}(\varepsilon). \tag{4.16}$$

Adicionalmente,

$$(\varepsilon - \varepsilon_j + i\eta)\,\tilde{\mathcal{G}}_{d_j d_j}(\varepsilon) = 1 - \frac{\Gamma}{1 + iV_{BT}\pi\rho_0}i\sum_l \tilde{\mathcal{G}}_{d_j d_l}(\varepsilon)$$

$$- \delta_{j1}\lambda\tilde{\mathcal{G}}_{\eta_1,d_j}(\varepsilon). \tag{4.17}$$

Usando

$$-\frac{\Gamma}{1 + iV_{BT}\pi\rho_0}i = -i\frac{\Gamma\left[1 - iV_{BT}\pi\rho_0\right]}{1 + (V_{BT}\pi\rho_0)^2} = -\frac{\Gamma}{1 + (V_{BT}\pi\rho_0)^2}i - \frac{\Gamma(V_{BT}\pi\rho_0)}{1 + (V_{BT}\pi\rho_0)^2}$$

$$= \overset{\sim}{\sum}^R + i\overset{\sim}{\sum}^I \tag{4.18}$$

na Eq. (4.17) com

$$\overset{\sim}{\sum}^I = -\tilde{\Gamma} = -\frac{\Gamma}{1 + (V_{LR}\pi\rho_0)^2} \tag{4.19}$$

e

$$\sum\tilde{}^{R} = -\frac{\Gamma\left(V_{BT}\pi\rho_0\right)}{1 + \left(V_{BT}\pi\rho_0\right)^2} \tag{4.20}$$

mostramos que

$$\left(\varepsilon - \tilde{\varepsilon}_j + i\tilde{\Gamma}\right)\tilde{\mathcal{G}}_{d_j d_j}\left(\varepsilon\right) = 1 + \left(\sum\tilde{}^{R} + i\sum\tilde{}^{I}\right)\sum_{l\neq j}\tilde{\mathcal{G}}_{d_j d_l}\left(\varepsilon\right) - \delta_{j1}\lambda\tilde{\mathcal{G}}_{\eta_1,d_j}\left(\varepsilon\right), \tag{4.21}$$

onde

$$\tilde{\varepsilon}_j = \varepsilon_j + \sum\tilde{}^{R} \tag{4.22}$$

é o nível renormalizado da energia para o QD. Repetimos a EOM para a FG

$$\mathcal{G}_{\eta_1,d_j}\left(t\right) = -\frac{i}{\hbar}\theta\left(t\right)\mathcal{Z}_e^{-1}\sum_n e^{-\beta E_n}\langle n|\left[\eta_1\left(t\right),d_j^\dagger\left(0\right)\right]_+|n\rangle = \frac{1}{\sqrt{2}}\mathcal{G}_{f,d_j}\left(t\right) + \frac{1}{\sqrt{2}}\mathcal{G}_{f^+,d_j}\left(t\right), \tag{4.23}$$

com

$$\mathcal{G}_{f,d_j}\left(t\right) = -\frac{i}{\hbar}\theta\left(t\right)\mathcal{Z}_e^{-1}\sum_n e^{-\beta E_n}\langle n|\left[f\left(t\right),d_j^\dagger\left(0\right)\right]_+|n\rangle \tag{4.24}$$

e

$$\mathcal{G}_{f^+,d_j}\left(t\right) = -\frac{i}{\hbar}\theta\left(t\right)\mathcal{Z}_e^{-1}\sum_n e^{-\beta E_n}\langle n|\left[f^\dagger\left(t\right),d_j^\dagger\left(0\right)\right]_+|n\rangle \tag{4.25}$$

para obter $\tilde{\mathcal{G}}_{\eta_1,d_j}\left(\varepsilon\right)$. Em coordenadas de energia, a Eq. (4.23) se reduz a

$$\tilde{\mathcal{G}}_{\eta_1,d_j}\left(\varepsilon\right) = \frac{1}{\sqrt{2}}\tilde{\mathcal{G}}_{f,d_j}\left(\varepsilon\right) + \frac{1}{\sqrt{2}}\tilde{\mathcal{G}}_{f^+,d_j}\left(\varepsilon\right). \tag{4.26}$$

Primeiro nós consideramos

$$\begin{aligned}
\frac{\partial}{\partial t}\mathcal{G}_{f,d_j}\left(t\right) &= -\frac{i}{\hbar}\delta\left(t\right)\mathcal{Z}_e^{-1}\sum_n e^{-\beta E_n}\langle n|\left[f\left(t\right),d_j^\dagger\left(0\right)\right]_+|n\rangle \\
&\quad + \left(-\frac{i}{\hbar}\right)\theta\left(t\right)\mathcal{Z}_e^{-1}\sum_n e^{-\beta E_n}\langle n|\left[\frac{\partial}{\partial t}f\left(t\right),d_j^\dagger\left(0\right)\right]_+|n\rangle
\end{aligned} \tag{4.27}$$

e

$$\begin{aligned}
\frac{\partial}{\partial t} f(t) &= -\frac{i}{\hbar}\left[f, \mathcal{H}_e\right] = -\frac{i}{\hbar}\left[f, \epsilon_M\left(f^\dagger f - \frac{1}{2}\right)\right] - \frac{i}{\hbar}\left[f, \frac{\lambda}{\sqrt{2}}\left(d_1 f^\dagger + d_1 f - d_1^\dagger f^\dagger - d_1^\dagger f\right)\right] \\
&= -\frac{i}{\hbar}\epsilon_M\left(ff^\dagger f - f^\dagger ff\right) - \frac{i}{\hbar}\frac{\lambda}{\sqrt{2}}\left\{fd_1 f^\dagger + fd_1 f - fd_1^\dagger f^\dagger - fd_1^\dagger f - d_1 f^\dagger f - d_1 ff + d_1^\dagger f^\dagger f + d_1^\dagger ff\right\} \\
&= -\frac{i}{\hbar}\epsilon_M\left(f - f^\dagger ff - f^\dagger ff\right) - \frac{i}{\hbar}\frac{\lambda}{\sqrt{2}}\left\{fd_1 f^\dagger - fd_1^\dagger f^\dagger - d_1 f^\dagger f + d_1^\dagger f^\dagger f\right\} \\
&= -\frac{i}{\hbar}\epsilon_M\left(f + f^\dagger ff - f^\dagger ff\right) - \frac{i}{\hbar}\frac{\lambda}{\sqrt{2}}\left\{fd_1 f^\dagger - d_1 f^\dagger f + d_1^\dagger f^\dagger f - fd_1^\dagger f^\dagger\right\} \\
&= -\frac{i}{\hbar}\epsilon_M f - \frac{i}{\hbar}\frac{\lambda}{\sqrt{2}}\left\{fd_1 f^\dagger - d_1 f^\dagger f + d_1^\dagger f^\dagger f + d_1^\dagger ff^\dagger\right\} \\
&= -\frac{i}{\hbar}\epsilon_M f - \frac{i}{\hbar}\frac{\lambda}{\sqrt{2}}\left\{-d_1\left(ff^\dagger + f^\dagger f\right) + d_1^\dagger\left(ff^\dagger + f^\dagger f\right)\right\} \\
&= -\frac{i}{\hbar}\epsilon_M f - \frac{i}{\hbar}\frac{\lambda}{\sqrt{2}}\left\{d_1^\dagger - d_1\right\},
\end{aligned} \tag{4.28}$$

que conduz a

$$\begin{aligned}
\frac{\partial}{\partial t}\mathcal{G}_{f,d_j}(t) &= -\frac{i}{\hbar}\delta(t)\,\mathcal{Z}_e^{-1}\sum_n e^{-\beta E_n}\langle n|\left[f(t), d_j^\dagger(0)\right]_+|n\rangle - \frac{i}{\hbar}\epsilon_M\left\{-\frac{i}{\hbar}\theta(t)\,\mathcal{Z}_e^{-1}\sum_n e^{-\beta E_n}\langle n|\left[f(t), d_j^\dagger(0)\right]_+|n\rangle\right\} \\
&\quad - \frac{i}{\hbar}\frac{\lambda}{\sqrt{2}}(-1)\left\{-\frac{i}{\hbar}\theta(t)\,\mathcal{Z}_e^{-1}\sum_n e^{-\beta E_n}\langle n|\left[d_1(t), d_j^\dagger(0)\right]_+|n\rangle\right\} \\
&\quad - \frac{i}{\hbar}\frac{\lambda}{\sqrt{2}}\left\{-\frac{i}{\hbar}\theta(t)\,\mathcal{Z}_e^{-1}\sum_n e^{-\beta E_n}\langle n|\left[d_1^\dagger(t), d_j^\dagger(0)\right]_+|n\rangle\right\} \\
&= -\frac{i}{\hbar}\delta(t)\,\mathcal{Z}_e^{-1}\sum_n e^{-\beta E_n}\langle n|\left[f(t), d_j^\dagger(0)\right]_+|n\rangle - \frac{i}{\hbar}\epsilon_M \mathcal{G}_{f,d_j}(t) - \frac{i}{\hbar}\frac{\lambda}{\sqrt{2}}(-1)\mathcal{G}_{d_1,d_j}(t) \\
&\quad - \frac{i}{\hbar}\frac{\lambda}{\sqrt{2}}\mathcal{G}_{d_1^+,d_j}(t).
\end{aligned} \tag{4.29}$$

De modo similar para a Eq. (4.25), nós escrevemos

$$\begin{aligned}
\frac{\partial}{\partial t}\mathcal{G}_{f^\dagger,d_j}(t) &= -\frac{i}{\hbar}\delta(t)\,\mathcal{Z}_e^{-1}\sum_n e^{-\beta E_n}\langle n|\left[f^\dagger(t), d_j^\dagger(0)\right]_+|n\rangle \\
&\quad + \left(-\frac{i}{\hbar}\right)\theta(t)\,\mathcal{Z}_e^{-1}\sum_n e^{-\beta E_n}\langle n|\left[\frac{\partial}{\partial t}f^\dagger(t), d_j^\dagger(0)\right]_+|n\rangle,
\end{aligned} \tag{4.30}$$

$$\frac{\partial}{\partial t} f^\dagger(t) = -\frac{i}{\hbar}\left[f^\dagger, \mathcal{H}_e\right] = -\frac{i}{\hbar}\left[f^\dagger, \epsilon_M\left(f^\dagger f - \frac{1}{2}\right)\right] - \frac{i}{\hbar}\left[f^\dagger, \frac{\lambda}{\sqrt{2}}\left(d_1 f^\dagger + d_1 f - d_1^\dagger f^\dagger - d_1^\dagger f\right)\right]$$

$$= -\frac{i}{\hbar}\epsilon_M\left(f^\dagger f^\dagger f - f^\dagger f f^\dagger\right)$$

$$\quad -\frac{i}{\hbar}\frac{\lambda}{\sqrt{2}}\left\{f^\dagger d_1 f^\dagger + f^\dagger d_1 f - f^\dagger d_1^\dagger f^\dagger - f^\dagger d_1^\dagger f - d_1 f^\dagger f^\dagger - d_1 f f^\dagger + d_1^\dagger f^\dagger f^\dagger + d_1^\dagger f f^\dagger\right\}$$

$$= -\frac{i}{\hbar}\epsilon_M\left(f^\dagger f^\dagger f - f^\dagger + f^\dagger f^\dagger f\right) - \frac{i}{\hbar}\frac{\lambda}{\sqrt{2}}\left\{f^\dagger d_1 f - f^\dagger d_1^\dagger f - d_1 f f^\dagger + d_1^\dagger f f^\dagger\right\}$$

$$= -\frac{i}{\hbar}\epsilon_M\left(-f^\dagger\right) - \frac{i}{\hbar}\frac{\lambda}{\sqrt{2}}\left\{d_1^\dagger\left(f f^\dagger + f^\dagger f\right) - d_1\left(f f^\dagger + f^\dagger f\right)\right\}$$

$$= -\frac{i}{\hbar}\epsilon_M\left(-f^\dagger\right) - \frac{i}{\hbar}\frac{\lambda}{\sqrt{2}}\left\{d_1^\dagger - d_1\right\} \tag{4.31}$$

e

$$\frac{\partial}{\partial t}\mathcal{G}_{f^\dagger,d_j}(t) = -\frac{i}{\hbar}\delta(t)\,\mathcal{Z}_e^{-1}\sum_n e^{-\beta E_n}\,\langle n|\left[f^\dagger(t), d_j^\dagger(0)\right]_+|n\rangle$$

$$\quad -\frac{i}{\hbar}\epsilon_M\left(-1\right)\left\{-\frac{i}{\hbar}\theta(t)\,\mathcal{Z}_e^{-1}\sum_n e^{-\beta E_n}\,\langle n|\left[f^\dagger(t), d_j^\dagger(0)\right]_+|n\rangle\right\}$$

$$\quad -\frac{i}{\hbar}\frac{\lambda}{\sqrt{2}}\left(-1\right)\left\{-\frac{i}{\hbar}\theta(t)\,\mathcal{Z}_e^{-1}\sum_n e^{-\beta E_n}\,\langle n|\left[d_1(t), d_j^\dagger(0)\right]_+|n\rangle\right\}$$

$$\quad -\frac{i}{\hbar}\frac{\lambda}{\sqrt{2}}\left\{-\frac{i}{\hbar}\theta(t)\,\mathcal{Z}_e^{-1}\sum_n e^{-\beta E_n}\,\langle n|\left[d_1^\dagger(t), d_j^\dagger(0)\right]_+|n\rangle\right\} \tag{4.32}$$

$$= -\frac{i}{\hbar}\delta(t)\,\mathcal{Z}_e^{-1}\sum_n e^{-\beta E_n}\,\langle n|\left[f^\dagger(t), d_j^\dagger(0)\right]_+|n\rangle - \frac{i}{\hbar}\epsilon_M\left(-1\right)\mathcal{G}_{f^\dagger,d_j}(t) - \frac{i}{\hbar}\frac{\lambda}{\sqrt{2}}\left(-1\right)\mathcal{G}_{d_1,d_j}(t)$$

$$\quad -\frac{i}{\hbar}\frac{\lambda}{\sqrt{2}}\mathcal{G}_{d_1^+,d_j}(t).$$

Tomando a transformada de Fourier no tempo nas Eqs. (4.26), (4.29) e (4.32), nós encontramos

$$(\varepsilon + i\eta)\tilde{\mathcal{G}}_{\eta_1,d_j}(\varepsilon) = \frac{1}{\sqrt{2}}(\varepsilon + i\eta)\tilde{\mathcal{G}}_{f,d_j}(\varepsilon) + \frac{1}{\sqrt{2}}(\varepsilon + i\eta)\tilde{\mathcal{G}}_{f^+,d_j}(\varepsilon), \tag{4.33}$$

$$(\varepsilon + i\eta)\tilde{\mathcal{G}}_{f,d_j}(\varepsilon) = \epsilon_M\tilde{\mathcal{G}}_{f,d_j}(\varepsilon) - \frac{\lambda}{\sqrt{2}}\tilde{\mathcal{G}}_{d_1,d_j}(\varepsilon) + \frac{\lambda}{\sqrt{2}}\tilde{\mathcal{G}}_{d_1^\dagger,d_j}(\varepsilon), \tag{4.34}$$

e

$$(\varepsilon + i\eta)\tilde{\mathcal{G}}_{f^\dagger,d_j}(\varepsilon) = -\epsilon_M\tilde{\mathcal{G}}_{f^\dagger,d_j}(\varepsilon) - \frac{\lambda}{\sqrt{2}}\tilde{\mathcal{G}}_{d_1,d_j}(\varepsilon) + \frac{\lambda}{\sqrt{2}}\tilde{\mathcal{G}}_{d_1^\dagger,d_j}(\varepsilon). \tag{4.35}$$

4.2   Sistema de um QD

Aqui nós fazemos $c_{eq} = c_q$ por simplicidade. Para um único QD, as Eqs. (4.21), (4.33), (4.35) tornam-se

$$\left(\varepsilon - \tilde{\varepsilon}_1 + i\tilde{\Gamma}\right)\tilde{\mathcal{G}}_{d_1 d_1}(\varepsilon) = 1 - \lambda\tilde{\mathcal{G}}_{\eta_1,d_1}(\varepsilon), \tag{4.36}$$

$$\tilde{\mathcal{G}}_{\eta_1,d_1}(\varepsilon) = \frac{1}{\sqrt{2}}\tilde{\mathcal{G}}_{f,d_1}(\varepsilon) + \frac{1}{\sqrt{2}}\tilde{\mathcal{G}}_{f+,d_1}(\varepsilon), \tag{4.37}$$

$$(\varepsilon + i\eta)\tilde{\mathcal{G}}_{f,d_1}(\varepsilon) = \epsilon_M\tilde{\mathcal{G}}_{f,d_1}(\varepsilon) - \frac{\lambda}{\sqrt{2}}\tilde{\mathcal{G}}_{d_1,d_1}(\varepsilon) + \frac{\lambda}{\sqrt{2}}\tilde{\mathcal{G}}_{d_1^\dagger,d_1}(\varepsilon), \tag{4.38}$$

e

$$(\varepsilon + i\eta)\tilde{\mathcal{G}}_{f^\dagger,d_1}(\varepsilon) = -\epsilon_M\tilde{\mathcal{G}}_{f^\dagger,d_1}(\varepsilon) - \frac{\lambda}{\sqrt{2}}\tilde{\mathcal{G}}_{d_1,d_1}(\varepsilon) + \frac{\lambda}{\sqrt{2}}\tilde{\mathcal{G}}_{d_1^\dagger,d_1}(\varepsilon). \tag{4.39}$$

Resolvendo as Eqs. (4.38) e (4.39) para $\tilde{\mathcal{G}}_{f,d_1}(\varepsilon)$ e $\tilde{\mathcal{G}}_{f^\dagger,d_1}(\varepsilon)$, encontramos

$$\tilde{\mathcal{G}}_{f,d_1}(\varepsilon) = -\frac{\frac{\lambda}{\sqrt{2}}\tilde{\mathcal{G}}_{d_1,d_1}(\varepsilon)}{(\varepsilon - \epsilon_M + i\eta)} + \frac{\frac{\lambda}{\sqrt{2}}\tilde{\mathcal{G}}_{d_1^\dagger,d_1}(\varepsilon)}{(\varepsilon - \epsilon_M + i\eta)} \tag{4.40}$$

e

$$\tilde{\mathcal{G}}_{f^\dagger,d_1}(\varepsilon) = -\frac{\frac{\lambda}{\sqrt{2}}\tilde{\mathcal{G}}_{d_1,d_1}(\varepsilon)}{(\varepsilon + \epsilon_M + i\eta)} + \frac{\frac{\lambda}{\sqrt{2}}\tilde{\mathcal{G}}_{d_1^\dagger,d_1}(\varepsilon)}{(\varepsilon + \epsilon_M + i\eta)}. \tag{4.41}$$

Nós precisamos encontrar $\tilde{\mathcal{G}}_{d_1^\dagger,d_1}(\varepsilon)$. Para fazer isto nós começamos com

$$\mathcal{G}_{d_1^\dagger,d_1}(t) = -\frac{i}{\hbar}\theta(t)\,\mathcal{Z}_e^{-1}\sum_n e^{-\beta E_n}\langle n|\left[d_1^\dagger(t), d_1^\dagger(0)\right]_+|n\rangle, \tag{4.42}$$

que conduz a

$$\frac{\partial}{\partial t}\mathcal{G}_{d_1^\dagger,d_1}(t) = -\frac{i}{\hbar}\delta(t)\,\mathcal{Z}_e^{-1}\sum_n e^{-\beta E_n}\langle n|\left[d_1^\dagger(t), d_1^\dagger(0)\right]_+|n\rangle$$
$$+ \left(-\frac{i}{\hbar}\right)\theta(t)\,\mathcal{Z}_e^{-1}\sum_n e^{-\beta E_n}\langle n|\left[\frac{\partial}{\partial t}d_1^\dagger(t), d_1^\dagger(0)\right]_+|n\rangle. \tag{4.43}$$

Nós substituímos

$$\frac{\partial}{\partial t}d_1^\dagger(t) = -\frac{i}{\hbar}\left[d_1^\dagger, \mathcal{H}_e\right] = -\frac{i}{\hbar}\left\{-\varepsilon_1 d_1^\dagger(t) - \sqrt{\frac{2}{\mathcal{N}}}V\sum_k c_k^\dagger(t) + \lambda\eta_1(t)\right\} \tag{4.44}$$

na Eq. (4.43) e obtemos

$$\frac{\partial}{\partial t}\mathcal{G}_{d_1^\dagger,d_1}(t) = -\frac{i}{\hbar}\delta(t)\,\mathcal{Z}_e^{-1}\sum_n e^{-\beta E_n}\langle n|\left[d_1^\dagger(t),d_1^\dagger(0)\right]_+|n\rangle$$

$$+\left(-\frac{i}{\hbar}\right)(-\varepsilon_1)\left\{-\frac{i}{\hbar}\theta(t)\,\mathcal{Z}_e^{-1}\sum_n e^{-\beta E_n}\langle n|\left[d_1^\dagger(t),d_1^\dagger(0)\right]_+|n\rangle\right\}$$

$$+\left(-\frac{i}{\hbar}\right)\left(-\sqrt{\frac{2}{\mathcal{N}}}V\right)\left\{-\frac{i}{\hbar}\theta(t)\,\mathcal{Z}_e^{-1}\sum_n e^{-\beta E_n}\langle n|\left[\sum_k c_k^\dagger(t),d_1^\dagger(0)\right]_+|n\rangle\right\}$$

$$+\left(-\frac{i}{\hbar}\right)\lambda\left\{-\frac{i}{\hbar}\theta(t)\,\mathcal{Z}_e^{-1}\sum_n e^{-\beta E_n}\langle n|\left[\eta_1(t),d_1^\dagger(0)\right]_+|n\rangle\right\}, \tag{4.45}$$

$$\frac{\partial}{\partial t}\mathcal{G}_{d_1^\dagger,d_1}(t) = -\frac{i}{\hbar}\delta(t)\,\mathcal{Z}_e^{-1}\sum_n e^{-\beta E_n}\langle n|\left[d_1^\dagger(t),d_1^\dagger(0)\right]_+|n\rangle$$

$$+\left(-\frac{i}{\hbar}\right)(-\varepsilon_1)\,\mathcal{G}_{d_1^\dagger,d_1}(t)-\left(\frac{i}{\hbar}\right)\left(-\sqrt{\frac{2}{\mathcal{N}}}V\right)\sum_k \mathcal{G}_{c_k^\dagger,d_1}(t)$$

$$+\left(-\frac{i}{\hbar}\right)\lambda\tilde{\mathcal{G}}_{\eta_1,d_1}(t), \tag{4.46}$$

que em coordenadas de energia torna-se

$$(\varepsilon+\varepsilon_1+i\eta)\tilde{\mathcal{G}}_{d_1^\dagger,d_1}(\varepsilon) = \left(-\sqrt{\frac{2}{\mathcal{N}}}V\right)\sum_k \mathcal{G}_{c_{ek}^\dagger,d_1}(\varepsilon)+\lambda\tilde{\mathcal{G}}_{\eta_1,d_1}(\varepsilon). \tag{4.47}$$

Podemos perceber que precisamos calcular $\sum_k \mathcal{G}_{c_{ek}^\dagger,d_1}$. Para fazer isso, vamos usar

$$\mathcal{G}_{c_{ek}^\dagger c_{eq}}(t) = -\frac{i}{\hbar}\theta(t)\,\mathcal{Z}_e^{-1}\sum_r e^{-\beta E_r}\langle r|\left[c_{ek}^\dagger(t),d_1^\dagger(0)\right]_+|r\rangle, \tag{4.48}$$

$$\frac{\partial}{\partial t}\mathcal{G}_{c_{ek}^\dagger,d_1}(t) = -\frac{i}{\hbar}\delta(t)\,\mathcal{Z}_e^{-1}\sum_n e^{-\beta E_n}\langle n|\left[c_{ek}^\dagger(t),d_1^\dagger(0)\right]_+|n\rangle$$

$$+\left(-\frac{i}{\hbar}\right)\theta(t)\,\mathcal{Z}_e^{-1}\sum_n e^{-\beta E_n}\langle n|\left[\frac{\partial}{\partial t}c_{ek}^\dagger(t),d_1^\dagger(0)\right]_+|n\rangle, \tag{4.49}$$

$$\frac{\partial}{\partial t}c_{ek}^\dagger(t) = -\frac{i}{\hbar}\left[c_{ek}^\dagger,\mathcal{H}_e\right] = \left(-\frac{i}{\hbar}\right)\left(-\varepsilon_k c_{ek}^\dagger(t)-\frac{\sqrt{2}}{\sqrt{\mathcal{N}}}V d_1^\dagger(t)-\frac{V_{BT}}{\mathcal{N}}\sum_p c_{ep}^\dagger(t)\right), \tag{4.50}$$

$$\frac{\partial}{\partial t}\mathcal{G}_{c_{ek}^\dagger, d_1}(t) = -\frac{i}{\hbar}\delta(t)\,\mathcal{Z}_e^{-1}\sum_n e^{-\beta E_n}\langle n|\left[c_{ek}^\dagger(t), d_1^\dagger(0)\right]_+ |n\rangle$$

$$+\left(-\frac{i}{\hbar}\right)(-\varepsilon_k)\left\{-\frac{i}{\hbar}\theta(t)\,\mathcal{Z}_e^{-1}\sum_n e^{-\beta E_n}\langle n|\left[c_{ek}^\dagger(t), d_1^\dagger(0)\right]_+ |n\rangle\right\}$$

$$+\left(-\frac{i}{\hbar}\right)\left(-\frac{\sqrt{2}}{\sqrt{\mathcal{N}}}V\right)\left\{-\frac{i}{\hbar}\theta(t)\,\mathcal{Z}_e^{-1}\sum_n e^{-\beta E_n}\langle n|\left[d_1^\dagger(t), d_1^\dagger(0)\right]_+ |n\rangle\right\}$$

$$+\left(-\frac{i}{\hbar}\right)\left(-\frac{V_{BT}}{\mathcal{N}}\right)\sum_p\left\{-\frac{i}{\hbar}\theta(t)\,\mathcal{Z}_e^{-1}\sum_n e^{-\beta E_n}\langle n|\left[c_{ep}^\dagger(t), d_1^\dagger(0)\right]_+ |n\rangle\right\}, \tag{4.51}$$

e

$$\frac{\partial}{\partial t}\mathcal{G}_{c_{ek}^\dagger, d_1}(t) = -\frac{i}{\hbar}\delta(t)\,\mathcal{Z}_e^{-1}\sum_n e^{-\beta E_n}\langle n|\left[c_{ek}^\dagger(t), d_1^\dagger(0)\right]_+ |n\rangle$$

$$+\left(-\frac{i}{\hbar}\right)(-\varepsilon_k)\,\mathcal{G}_{c_{ek}^\dagger, d_1}(t) + \left(-\frac{i}{\hbar}\right)\left(-\frac{\sqrt{2}}{\sqrt{\mathcal{N}}}V\right)\tilde{\mathcal{G}}_{d_1^\dagger, d_1}(t)$$

$$+\left(-\frac{i}{\hbar}\right)\left(-\frac{V_{BT}}{\mathcal{N}}\right)\sum_p \tilde{\mathcal{G}}_{c_{ep}^\dagger, d_1}(t). \tag{4.52}$$

Tomando a transformada de Fourier na Eq. (4.52), temos

$$(\varepsilon + i\eta)\,\tilde{\mathcal{G}}_{c_{ek}^\dagger, d_1}(\varepsilon) = -\varepsilon_k\mathcal{G}_{c_{ek}^\dagger, d_1}(t) - \frac{\sqrt{2}}{\sqrt{\mathcal{N}}}V\tilde{\mathcal{G}}_{d_1^\dagger, d_1}(\varepsilon) - \frac{V_{BT}}{\mathcal{N}}\sum_p \tilde{\mathcal{G}}_{c_{ep}^\dagger, d_1}(\varepsilon), \tag{4.53}$$

$$(\varepsilon + \varepsilon_k + i\eta)\,\tilde{\mathcal{G}}_{c_{ek}^\dagger, d_1}(\varepsilon) = -\frac{\sqrt{2}}{\sqrt{\mathcal{N}}}V\tilde{\mathcal{G}}_{d_1^\dagger, d_1}(\varepsilon) - \frac{V_{BT}}{\mathcal{N}}\sum_p \tilde{\mathcal{G}}_{c_{ep}^\dagger, d_1}(\varepsilon), \tag{4.54}$$

$$\tilde{\mathcal{G}}_{c_{ek}^\dagger, d_1}(\varepsilon) = -\frac{\frac{\sqrt{2}}{\sqrt{\mathcal{N}}}V\tilde{\mathcal{G}}_{d_1^\dagger, d_1}(\varepsilon)}{(\varepsilon + \varepsilon_k + i\eta)} - \frac{\frac{V_{BT}}{\mathcal{N}}\sum_p \tilde{\mathcal{G}}_{c_{ep}^\dagger, d_1}(\varepsilon)}{(\varepsilon + \varepsilon_k + i\eta)}, \tag{4.55}$$

$$\sum_k \tilde{\mathcal{G}}_{c_{ek}^\dagger, d_1}(\varepsilon) = -\sum_k \frac{\frac{\sqrt{2}}{\sqrt{\mathcal{N}}}V\tilde{\mathcal{G}}_{d_1^\dagger, d_1}(\varepsilon)}{(\varepsilon + \varepsilon_k + i\eta)} - \sum_k \frac{\frac{V_{BT}}{\mathcal{N}}\sum_p \tilde{\mathcal{G}}_{c_{ep}^\dagger, d_1}(\varepsilon)}{(\varepsilon + \varepsilon_k + i\eta)}, \tag{4.56}$$

e

$$\sum_k \tilde{\mathcal{G}}_{c_{ek}^\dagger, d_1}(\varepsilon) = -\frac{\frac{\sqrt{2}}{\sqrt{\mathcal{N}}}V\sum_k \frac{1}{(\varepsilon + \varepsilon_k + i\eta)}}{1 + \frac{V_{BT}}{\mathcal{N}}\sum_k \frac{1}{(\varepsilon + \varepsilon_k + i\eta)}}\tilde{\mathcal{G}}_{d_1^\dagger, d_1}(\varepsilon). \tag{4.57}$$

Substituindo as Eq. (4.57) e (4.37) na Eq. (4.47) encontramos

$$\left(\varepsilon + \varepsilon_1 + i\eta\right)\tilde{\mathcal{G}}_{d_1^\dagger, d_1}\left(\varepsilon\right) = \left(\sqrt{2}V\right)^2 \frac{\frac{1}{\mathcal{N}}\sum_k \frac{1}{(\varepsilon+\varepsilon_k+i\eta)}}{1 + \frac{V_{BT}}{\mathcal{N}}\sum_k \frac{1}{(\varepsilon+\varepsilon_k+i\eta)}}\tilde{\mathcal{G}}_{d_1^\dagger, d_1}\left(\varepsilon\right) + \lambda\tilde{\mathcal{G}}_{\eta_1, d_1}\left(\varepsilon\right)$$

$$= \left(\sqrt{2}V\right)^2 \frac{\frac{1}{\mathcal{N}}\sum_k \frac{1}{(\varepsilon+\varepsilon_k+i\eta)}}{1 + \frac{V_{BT}}{\mathcal{N}}\sum_k \frac{1}{(\varepsilon+\varepsilon_k+i\eta)}}\tilde{\mathcal{G}}_{d_1^\dagger, d_1}\left(\varepsilon\right)$$

$$+ \lambda\frac{1}{\sqrt{2}}\tilde{\mathcal{G}}_{f, d_1} + \lambda\frac{1}{\sqrt{2}}\tilde{\mathcal{G}}_{f^+, d_1}\left(\varepsilon\right), \tag{4.58}$$

$$\left(\varepsilon + \tilde{\varepsilon}_1 + i\tilde{\Gamma}\right)\tilde{\mathcal{G}}_{d_1^\dagger, d_1}\left(\varepsilon\right) = \lambda\frac{1}{\sqrt{2}}\tilde{\mathcal{G}}_{f, d_1} + \lambda\frac{1}{\sqrt{2}}\tilde{\mathcal{G}}_{f^+, d_1}\left(\varepsilon\right), \tag{4.59}$$

onde nós usamos

$$\frac{\left(\sqrt{2}V\right)^2 \frac{1}{\mathcal{N}}\sum_k \frac{1}{(\varepsilon+\varepsilon_k+i\eta)}}{1 + \frac{V_{BT}}{\mathcal{N}}\sum_k \frac{1}{(\varepsilon+\varepsilon_k+i\eta)}} = -\frac{i\Gamma}{1 - iV_{BT}\pi\rho_0} = -\frac{\left(1 + iV_{BT}\pi\rho_0\right)}{1 + \left(V_{BT}\pi\rho_0\right)^2}i\Gamma$$

$$= -i\frac{\Gamma}{1 + \left(V_{BT}\pi\rho_0\right)^2} + \frac{V_{BT}\pi\rho_0\Gamma}{1 + \left(V_{BT}\pi\rho_0\right)^2}$$

$$= -i\tilde{\Gamma} - \overset{\sim}{\sum}^R \tag{4.60}$$

com a Eq. (4.22). Substituindo as Eqs. (4.40) e (4.41) na Eq. (4.59), mostramos que

$$\left(\varepsilon + \tilde{\varepsilon}_1 + i\tilde{\Gamma}\right)\tilde{\mathcal{G}}_{d_1^\dagger, d_1}\left(\varepsilon\right) = -\frac{\lambda^2}{2}\frac{1}{\left(\varepsilon - \epsilon_M + i\eta\right)}\tilde{\mathcal{G}}_{d_1, d_1}\left(\varepsilon\right)$$

$$+ \frac{\lambda^2}{2}\frac{1}{\left(\varepsilon - \epsilon_M + i\eta\right)}\tilde{\mathcal{G}}_{d_1^\dagger, d_1}\left(\varepsilon\right)$$

$$- \frac{\lambda^2}{2}\frac{1}{\left(\varepsilon + \epsilon_M + i\eta\right)}\tilde{\mathcal{G}}_{d_1, d_1}\left(\varepsilon\right)$$

$$+ \frac{\lambda^2}{2}\frac{1}{\left(\varepsilon + \epsilon_M + i\eta\right)}\tilde{\mathcal{G}}_{d_1^\dagger, d_1}\left(\varepsilon\right)$$

$$= \lambda^2 K\left(\varepsilon\right)\tilde{\mathcal{G}}_{d_1^\dagger, d_1}\left(\varepsilon\right) - \lambda^2 K\left(\varepsilon\right)\tilde{\mathcal{G}}_{d_1, d_1}\left(\varepsilon\right)$$

$$\left(\varepsilon + \tilde{\varepsilon}_1 + i\tilde{\Gamma} - \lambda^2 K\left(\varepsilon\right)\right)\tilde{\mathcal{G}}_{d_1^\dagger, d_1}\left(\varepsilon\right) = -\lambda^2 K\left(\varepsilon\right)\tilde{\mathcal{G}}_{d_1, d_1}\left(\varepsilon\right), \tag{4.61}$$

$$\tilde{\mathcal{G}}_{d_1^\dagger, d_1}\left(\varepsilon\right) = -\frac{\lambda^2 K\left(\varepsilon\right)}{\left(\varepsilon + \tilde{\varepsilon}_1 + i\tilde{\Gamma} - \lambda^2 K\left(\varepsilon\right)\right)}\tilde{\mathcal{G}}_{d_1, d_1}\left(\varepsilon\right) \tag{4.62}$$

com

$$\frac{\lambda^2}{2}\left\{\frac{1}{\left(\varepsilon + \epsilon_M + i\eta\right)} + \frac{1}{\left(\varepsilon - \epsilon_M + i\eta\right)}\right\} = \frac{\lambda^2}{2}\frac{2\varepsilon}{\left(\varepsilon + \epsilon_M + i\eta\right)\left(\varepsilon - \epsilon_M + i\eta\right)}$$

$$= \frac{\lambda^2}{2}\frac{2\varepsilon}{\left(\varepsilon + \epsilon_M\right)\left(\varepsilon - \epsilon_M\right)}$$

$$= \frac{\lambda^2}{2}\frac{2\varepsilon}{\left(\varepsilon^2 - \epsilon_M^2\right)} = \lambda^2\frac{\varepsilon}{\left(\varepsilon^2 - \epsilon_M^2\right)}$$

$$= \lambda^2\frac{1}{\varepsilon - \frac{\epsilon_M^2}{\varepsilon}} = \lambda^2 K\left(\varepsilon\right). \tag{4.63}$$

Das Eqs. (4.36), (4.37), (4.40), (4.41), (4.62) e (4.63) nós podemos escrever

$$\left(\varepsilon - \tilde{\varepsilon}_1 + i\tilde{\Gamma}\right)\tilde{\mathcal{G}}_{d_1 d_1}(\varepsilon) = 1 - \lambda\tilde{\mathcal{G}}_{\eta_1,d_1}(\varepsilon),$$

$$= 1 - \frac{\lambda}{\sqrt{2}}\tilde{\mathcal{G}}_{f,d_1}(\varepsilon) - \frac{\lambda}{\sqrt{2}}\tilde{\mathcal{G}}_{f^+,d_1}(\varepsilon)$$

$$= 1 + \frac{\lambda^2}{2}\frac{\tilde{\mathcal{G}}_{d_1,d_1}(\varepsilon)}{(\varepsilon - \epsilon_M + i\eta)} - \frac{\lambda^2}{2}\frac{\tilde{\mathcal{G}}_{d_1^\dagger,d_1}(\varepsilon)}{(\varepsilon - \epsilon_M + i\eta)}$$

$$+ \frac{\lambda^2}{2}\frac{\tilde{\mathcal{G}}_{d_1,d_1}(\varepsilon)}{(\varepsilon + \epsilon_M + i\eta)} - \frac{\lambda^2}{2}\frac{\tilde{\mathcal{G}}_{d_1^\dagger,d_1}(\varepsilon)}{(\varepsilon + \epsilon_M + i\eta)}$$

$$= 1 + \lambda^2 K(\varepsilon)\tilde{\mathcal{G}}_{d_1,d_1}(\varepsilon) - \lambda^2 K(\varepsilon)\tilde{\mathcal{G}}_{d_1^\dagger,d_1}(\varepsilon)$$

$$= 1 + \lambda^2 K(\varepsilon)\tilde{\mathcal{G}}_{d_1,d_1}(\varepsilon)$$

$$- \lambda^2 K(\varepsilon)\left\{-\frac{\lambda^2 K(\varepsilon)}{\left(\varepsilon + \tilde{\varepsilon}_1 + i\tilde{\Gamma} - \lambda^2 K(\varepsilon)\right)}\tilde{\mathcal{G}}_{d_1,d_1}(\varepsilon)\right\}$$

$$= 1 + \lambda^2 K(\varepsilon)\tilde{\mathcal{G}}_{d_1,d_1}(\varepsilon) + \lambda^2 K(\varepsilon)\lambda^2\tilde{K}(\varepsilon)\tilde{\mathcal{G}}_{d_1,d_1}(\varepsilon)$$

$$= 1 + \lambda^2 K(\varepsilon)\left(1 + \lambda^2\tilde{K}(\varepsilon)\right)\tilde{\mathcal{G}}_{d_1,d_1}(\varepsilon), \qquad (4.64)$$

com

$$\tilde{K}(\varepsilon) = \frac{K(\varepsilon)}{\left(\varepsilon + \tilde{\varepsilon}_1 + i\tilde{\Gamma} - \lambda^2 K(\varepsilon)\right)}. \qquad (4.65)$$

Finalmente, a FG do QD é

$$\tilde{\mathcal{G}}_{d_1,d_1}(\varepsilon) = \frac{1}{\varepsilon - \tilde{\varepsilon}_1 + i\tilde{\Gamma} - \lambda^2 K(\varepsilon)\left[1 + \lambda^2\tilde{K}(\varepsilon)\right]}. \qquad (4.66)$$

Capítulo 5

Quantum dots (QDs) em série

Abaixo, descrevemos teoricamente a configuração da Fig. 1.1(a) com uma cadeia topológica de Kitaev acoplada a dois QDs hibridizados com terminais metálicos [33, 36]. O esboço simplificado de tal sistema é representado na Fig. 1.1(b), que é governado pelo Hamiltoniano

$$
\begin{aligned}
\mathcal{H}_{\text{Full}} &= \sum_{\alpha \mathbf{k}} \tilde{\varepsilon}_{\alpha \mathbf{k}} c_{\alpha \mathbf{k}}^{\dagger} c_{\alpha \mathbf{k}} + \sum_{\alpha} \varepsilon_{\alpha} d_{\alpha}^{\dagger} d_{\alpha} + T_{\text{c}} (d_{L}^{\dagger} d_{R} + \text{H.c.}) \\
&+ \mathcal{V} \sum_{\alpha \mathbf{k}} (c_{\alpha \mathbf{k}}^{\dagger} d_{\alpha} + \text{H.c.}) + \mathcal{H}_{\text{MFs}},
\end{aligned}
\tag{5.1}
$$

onde os elétrons dos terminais $\alpha = L, R$ são descritos pelos operadores $c_{\alpha \mathbf{k}}^{\dagger}$ ($c_{\alpha \mathbf{k}}$) para criação(aniquilação) de um elétron no estado quântico descrito por um número de onda $\mathbf{k}$ e energia $\tilde{\varepsilon}_{\alpha \mathbf{k}} = \tilde{\varepsilon}_{\mathbf{k}} - \mu_{\alpha}$, com potencial químico μ_{α}. Para os QDs acoplados aos terminais, $d_{\alpha}^{\dagger}$ (d_{α}) é para criação (aniquilação) de um elétron no estado ε_{α}. O acoplamento entre os QDs esquerdo-direito é T_{c}, $\mathcal{V}$ representa a hibridização entre esses QDs e os terminais. Acerca do $\mathcal{H}_{\text{MFs}}$ nos referimos à Ref.[33], que discute os QDs com grande espaçamento de energia entre os níveis de spins-up e down devido à separação Zeeman. Consequentemente, a condição *spinless* é cumprida onde um único estado de spin é relevante para a supercondutividade topológica emergente. Desta forma, nossos QDs não dependem da energia de Coulomb, como nas Refs.[9],[37], portanto, os QDs apenas se acoplam de forma assimétrica à cadeia Kitaev com amplitudes complexas de tunelamento λ_{L} e λ_{R}, respectivamente, para os QDs esquerdo e direito, como segue

$$
\begin{aligned}
\mathcal{H}_{\text{MFs}} &= i \varepsilon_{M} \Psi_{1} \Psi_{2} + |\lambda_{R}| (e^{i \phi_{R}} d_{R} - e^{-i \phi_{R}} d_{R}^{\dagger}) \Psi_{1} \\
&+ |\lambda_{L}| (e^{i \phi_{L}} d_{L} - e^{-i \phi_{L}} d_{L}^{\dagger}) \Psi_{1},
\end{aligned}
\tag{5.2}
$$

onde $\Psi_{1} = \Psi_{1}^{\dagger}$ e $\Psi_{2} = \Psi_{2}^{\dagger}$ descrevem os MFs localizados nas bordas do fio com um termo de sobreposição $\varepsilon_{M} \sim e^{-L/\xi}$, onde o L e ξ designam, respectivamente, o tamanho da cadeia Kitaev e o comprimento de coerência do supercondutor.

Por uma questão de simplicidade, empregamos as seguintes substituições $d_{L} = e^{-i \phi_{L}} [(\cos \theta) \tilde{d}_{\uparrow} -$

$(\sin\theta)\,\tilde{d}_\downarrow]$, $d_R = e^{-i\phi_R}[(\sin\theta)\,\tilde{d}_\uparrow+(\cos\theta)\,\tilde{d}_\downarrow]$, $c_{\mathbf{k}L} = e^{-i\phi_L}[(\cos\theta)\,\tilde{c}_{\mathbf{k}\uparrow}-(\sin\theta)\,\tilde{c}_{\mathbf{k}\downarrow}]$ e $c_{\mathbf{k}R} = e^{-i\phi_R}[(\sin\theta)\,\tilde{c}_{\mathbf{k}\uparrow}+$ $(\cos\theta)\,\tilde{c}_{\mathbf{k}\downarrow}]$ no Hamiltoniano da Eq.(5.1), em particular no regime de voltagem zero ($\mu_\alpha = 0 \equiv$ nível de Fermi dos terminais), para obter:

$$
\begin{aligned}
\mathcal{H}_{\text{Full}} &= \sum_{\mathbf{k},\sigma}\tilde{\varepsilon}_{\mathbf{k}}\tilde{c}^\dagger_{\mathbf{k}\sigma}\tilde{c}_{\mathbf{k}\sigma} + \sum_\sigma \epsilon_{d\sigma}\tilde{d}^\dagger_\sigma\tilde{d}_\sigma + \mathcal{V}\sum_{\mathbf{k},\sigma}(\tilde{c}^\dagger_{\mathbf{k}\sigma}\tilde{d}_\sigma + \text{H.c.}) \\
&+ \mathcal{H}_{\text{MFs}},
\end{aligned}
\tag{5.3}
$$

o qual emula um único QD efetivo acoplado a um único terminal ambos exibindo um grau de liberdade de spin artificial $\sigma = \pm 1$ ($\uparrow,\downarrow$) (see Fig. 1.1(c) para tal representação). Chamamos a atenção que, a partir de agora, rotulamos a variável acima mencionada por *pseudospin*(transformação utilizada para representar os níveis de energia dos QDs em uma nova base de senos e cossenos).

Como na Ref.[33], nós temos proteção topológica de nossas descobertas se a diferença de fase $\phi_L-\phi_R = 2n\pi$, com n inteiro sendo ajustável através do fluxo magnético, levando em consideração $\cos(2\theta) = \frac{\triangle\epsilon\cos(\phi_L-\phi_R)}{\sqrt{4(T_c)^2+(\triangle\epsilon)^2}}$, $\triangle\epsilon = \varepsilon_L - \varepsilon_R$ como o *detuning* dos QDs originais *spinless*, o desdobramento (hiato) *pseudo*-Zeeman $\epsilon_{d\uparrow} - \epsilon_{d\downarrow}$, com $\epsilon_{d\sigma} = \frac{(\varepsilon_L+\varepsilon_R)}{2} + \frac{\sigma}{2}\sqrt{4(T_c)^2 + (\triangle\epsilon)^2}$ e

$$
\mathcal{H}_{\text{MFs}} = \varepsilon_M(\eta^\dagger_\uparrow\eta_\uparrow - \frac{1}{2}) + \sum_\sigma \bar{\lambda}_\sigma(\tilde{d}_\sigma\eta^\dagger_\uparrow + \tilde{d}_\sigma\eta_\uparrow + \text{H.c.}),
\tag{5.4}
$$

onde usamos $\Psi_1 = \frac{1}{\sqrt{2}}\left(\eta^\dagger_\uparrow + \eta_\uparrow\right)$ e $\Psi_2 = \frac{i}{\sqrt{2}}\left(\eta^\dagger_\uparrow - \eta_\uparrow\right)$ para construir o *qubit* $\eta_\uparrow$ composto por MFs, com $\bar{\lambda}_\uparrow = \frac{1}{\sqrt{2}}(|\lambda_L|\cos\theta+|\lambda_R|\sin\theta)$ e $\bar{\lambda}_\downarrow = \frac{1}{\sqrt{2}}(|\lambda_R|\cos\theta-|\lambda_L|\sin\theta)$. Como resultado, o hiato *pseudo*-Zeeman começa a ser renormalizado pela interação com as demais partes do sistema, isto é, $\tilde{\epsilon}_{d\uparrow} - \tilde{\epsilon}_{d\downarrow}$ no lugar de $\epsilon_{d\uparrow} - \epsilon_{d\downarrow}$.

Chamamos a atenção para o mapeamento do sistema Hamiltoniano na Eq. (5.4), onde se pode reconhecer que o dispositivo da Fig. 1.1(b) é equivalente ao QD $\tilde{d}_\sigma$ simulando os dois QDs da esquerda e direita sem spin, em particular acoplados lateralmente à $\eta_\uparrow$, o que corresponde a um QD que substitui a cadeia Kitaev. Isso abre a possibilidade de reproduzir experimentalmente o mesmo fenômeno relatado aqui para a cadeia topológica de Kitaev empregando QDs, mas na presença de um par de Cooper dividido em $\tilde{d}_\sigma$ e $\eta_\uparrow$ com amplitude de pareamento $\bar{\lambda}_\sigma$ como os termos $\bar{\lambda}_\sigma(\tilde{d}_\sigma\eta_\uparrow + \text{H.c.})$ apontam. Além disso, o tunelamento normal entre esses QDs também deve ser igual à $\bar{\lambda}_\sigma$, ou seja, $\bar{\lambda}_\sigma(\tilde{d}_\sigma\eta^\dagger_\uparrow + \text{H.c.})$, apenas para garantir o surgimento de um *qubit* de MFs no chamado *sweet spot* como previsto na Ref.[38]. Em tal trabalho, a equivalência da cadeia topológica de Kitaev com um sistema de QDs é estabelecida por meio de um Hamiltoniano análogo à nossa Eq. (5.4). Desta forma, este sistema de QDs que hospeda MFs torna-se uma alternativa experimental com respeito à cadeia topológica de Kitaev.

No que se segue, utilizamos a fórmula de Landauer-Büttiker para a condutância $\mathcal{G}$[35] para analisar o transporte através dos QDs, que é

$$\mathcal{G} = \frac{e^2}{h} \int d\varepsilon \left(-\frac{\partial f_F}{\partial \varepsilon} \right) \mathcal{T}_{\text{Total}}, \tag{5.5}$$

onde f_F representa a distribuição de Fermi-Dirac, $\mathcal{T}_{\text{Total}} = \sum_j \mathcal{T}_{jj} + \sum_j \mathcal{T}_{j\bar{j}}$ é a transmitância total com $j = L, R$ respectivamente para $\bar{j} = R, L$ para correlacionar QDs distintos, no qual $\mathcal{T}_{jl} = \mathcal{T}_{\uparrow\uparrow} + \mathcal{T}_{\downarrow\downarrow} + \mathcal{T}_{\uparrow\downarrow} + \mathcal{T}_{\downarrow\uparrow}$ detecta a transmitância através dos canais $l, j = L, R$ em termos dos coeficientes $\mathcal{T}_{\sigma\tilde{\sigma}}$ para a representação do *pseudospin*.

Além disso, $\mathcal{T}_{jl} = \pi\Gamma\rho_{jl}$ depende do alargamento de Anderson $\Gamma = \pi\mathcal{V}^2 \sum_{\mathbf{k}} \delta(\varepsilon - \tilde{\varepsilon}_{\mathbf{k}})$ [34] e $\rho_{jl} = (-1/\pi)\text{Im}(\tilde{\mathcal{G}}_{d_j,d_l})$ como a densidade de estados para os QDs sem spin do Hamiltoniano da Eq.(5.1) a partir da função de Green retardada $\tilde{\mathcal{G}}_{d_j,d_l}$, que é dada por

$$\rho_{LL} = -\frac{1}{\pi}\text{Im}\{\cos^2\theta\tilde{\mathcal{G}}_{\tilde{d}_\uparrow,\tilde{d}_\uparrow} + \sin^2\theta\tilde{\mathcal{G}}_{\tilde{d}_\downarrow,\tilde{d}_\downarrow}$$
$$- \sin\theta\cos\theta(\tilde{\mathcal{G}}_{\tilde{d}_\downarrow,\tilde{d}_\uparrow} + \tilde{\mathcal{G}}_{\tilde{d}_\uparrow,\tilde{d}_\downarrow})\}, \tag{5.6}$$

$$\rho_{RR} = -\frac{1}{\pi}\text{Im}\{\sin^2\theta\tilde{\mathcal{G}}_{\tilde{d}_\uparrow,\tilde{d}_\uparrow} + \cos^2\theta\tilde{\mathcal{G}}_{\tilde{d}_\downarrow,\tilde{d}_\downarrow}$$
$$+ \sin\theta\cos\theta(\tilde{\mathcal{G}}_{\tilde{d}_\downarrow,\tilde{d}_\uparrow} + \tilde{\mathcal{G}}_{\tilde{d}_\uparrow,\tilde{d}_\downarrow})\}, \tag{5.7}$$

$$\rho_{RL} = -\frac{1}{\pi}\text{Im}\{\sin\theta\cos\theta(\tilde{\mathcal{G}}_{\tilde{d}_\uparrow,\tilde{d}_\uparrow} - \tilde{\mathcal{G}}_{\tilde{d}_\downarrow,\tilde{d}_\downarrow})$$
$$+ \cos^2\theta\tilde{\mathcal{G}}_{\tilde{d}_\downarrow,\tilde{d}_\uparrow} - \sin^2\theta\tilde{\mathcal{G}}_{\tilde{d}_\uparrow,\tilde{d}_\downarrow}\} \tag{5.8}$$

e

$$\rho_{LR} = -\frac{1}{\pi}\text{Im}\{\sin\theta\cos\theta(\tilde{\mathcal{G}}_{\tilde{d}_\uparrow,\tilde{d}_\uparrow} - \tilde{\mathcal{G}}_{\tilde{d}_\downarrow,\tilde{d}_\downarrow})$$
$$- \sin^2\theta\tilde{\mathcal{G}}_{\tilde{d}_\downarrow,\tilde{d}_\uparrow} + \cos^2\theta\tilde{\mathcal{G}}_{\tilde{d}_\uparrow,\tilde{d}_\downarrow}\}, \tag{5.9}$$

em termos das funções de Green retardadas $\tilde{\mathcal{G}}_{\tilde{d}_\sigma,\tilde{d}_{\tilde{\sigma}}}$ na representação do *pseudospin*. Para avaliar $\tilde{\mathcal{G}}_{\tilde{d}_\sigma,\tilde{d}_{\tilde{\sigma}}}$, nós devemos empregar o método da equação de movimento [35] usando as Eqs.(5.3) and (5.4). Começamos definindo a função de Green retardada para o QD, no domínio do tempo t como segue:

$$\mathcal{G}_{\tilde{d}_\gamma,\tilde{d}_\sigma}(t) = -\frac{i}{\hbar}\theta(t)\,\text{Tr}\{\rho[\tilde{d}_\gamma(t), \tilde{d}_\sigma^\dagger(0)]_+\}, \tag{5.10}$$

onde $\theta(t)$ é a função degrau e ρ é a matriz densidade do Hamiltoniano. Seguindo o procedimento de EOM, evoluímos:

$$i\hbar\frac{\partial}{\partial t}\mathcal{G}_{\tilde{d}_\gamma,\tilde{d}_\sigma}(t) = \delta(t)\,\text{Tr}\{\rho[\tilde{d}_\gamma(t), \tilde{d}_\sigma^\dagger(0)]_+\} + \theta(t)\,\text{Tr}\{\rho[\frac{\partial}{\partial t}\tilde{d}_\gamma(t), \tilde{d}_\sigma^\dagger(0)]_+\}, \tag{5.11}$$

com $\delta(t)$ sendo a função delta de Dirac. De acordo com a equação de Heisenberg, obtemos a evolução no

tempo do operador $\tilde{d}_\gamma(t)$:

$$\frac{\partial}{\partial t}\tilde{d}_\gamma(t) \;=\; -\frac{i}{\hbar}[\tilde{d}_\gamma, \mathcal{H}_{\text{Full}}] = -\frac{i}{\hbar}(\varepsilon_{d,\gamma}\tilde{d}_\gamma + \mathcal{V}\sum_{\mathbf{k}}\tilde{c}_{\gamma\mathbf{k}} - \bar{\lambda}_\gamma\eta - \bar{\lambda}_\gamma\eta^\dagger). \tag{5.12}$$

Substituindo Eq.(5.12) na Eq.(5.11), nós encontramos[1]:

$$
\begin{aligned}
i\hbar\frac{\partial}{\partial t}\mathcal{G}_{\tilde{d}_\gamma,\tilde{d}_\sigma}(t) \;=\;& \delta(t)\,\mathrm{Tr}\{\rho[\tilde{d}_\gamma(t),\tilde{d}_\sigma^\dagger(0)]_+\} + \varepsilon_{d,\gamma}(-\frac{i}{\hbar})\theta(t)\,\mathrm{Tr}\{\rho[\tilde{d}_\gamma(t),\tilde{d}_\sigma^\dagger(0)]_+\} \\
&+ \mathcal{V}\sum_{\mathbf{k}}(-\frac{i}{\hbar})\theta\,\mathrm{Tr}\{\rho[\tilde{c}_{\gamma\mathbf{k}}(t),\tilde{d}_\sigma^\dagger(0)]_+\} - \bar{\lambda}_\gamma(-\frac{i}{\hbar})\theta(t)\,\mathrm{Tr}\{\rho[\eta(t),\tilde{d}_\sigma^\dagger(0)]_+\} \\
&- \bar{\lambda}_\gamma(-\frac{i}{\hbar})\theta(t)\,\mathrm{Tr}\{\rho[\eta^\dagger(t),\tilde{d}_\sigma^\dagger(0)]_+\}.
\end{aligned}
\tag{5.13}
$$

Temos então:

$$i\hbar\frac{\partial}{\partial t}\mathcal{G}_{\tilde{d}_\gamma,\tilde{d}_\sigma}(t) \;=\; \delta(t)\,\mathrm{Tr}\{\rho[\tilde{d}_\gamma(t),\tilde{d}_\sigma^\dagger(0)]_+\} + \varepsilon_{d,\gamma}\mathcal{G}_{\tilde{d}_\gamma,\tilde{d}_\sigma}(t) + \mathcal{V}\sum_{\mathbf{k}}\mathcal{G}_{\tilde{c}_{\gamma\mathbf{k}},\tilde{d}_\sigma}(t) - \bar{\lambda}_\gamma\mathcal{G}_{\eta,\tilde{d}_\sigma}(t) - \bar{\lambda}_\gamma\mathcal{G}_{\eta^\dagger,\tilde{d}_\sigma}(t) \tag{5.14}$$

Aplicando a transformada de Fourier no domínio da energia [2] ε na Eq.(5.14), encontramos:

$$(\varepsilon - \varepsilon_{d,\gamma})\tilde{\mathcal{G}}_{\tilde{d}_\gamma,\tilde{d}_\sigma}(\varepsilon) \;=\; \delta_{\sigma\gamma} + \mathcal{V}\sum_{\mathbf{k}}\tilde{\mathcal{G}}_{\tilde{c}_{\gamma\mathbf{k}},\tilde{d}_\sigma}(\varepsilon) - \bar{\lambda}_\gamma\tilde{\mathcal{G}}_{\eta,\tilde{d}_\sigma}(\varepsilon) - \bar{\lambda}_\gamma\tilde{\mathcal{G}}_{\eta^\dagger,\tilde{d}_\sigma}(\varepsilon). \tag{5.15}$$

Agora, nós devemos calcular $\tilde{\mathcal{G}}_{\tilde{c}_{\gamma\mathbf{k}},\tilde{d}_\sigma}(\varepsilon)$, definida no tempo como:

$$\mathcal{G}_{\tilde{c}_{\gamma\mathbf{k}},\tilde{d}_\sigma}(t) = -\frac{i}{\hbar}\theta(t)\,\mathrm{Tr}\{\rho[\tilde{c}_{\gamma\mathbf{k}}(t),\tilde{d}_\sigma^\dagger(0)]_+\}, \tag{5.16}$$

com a derivação no tempo dá:

$$i\hbar\frac{\partial}{\partial t}\mathcal{G}_{\tilde{c}_{\gamma\mathbf{k}},\tilde{d}_\sigma}(t) \;=\; \delta(t)\,\mathrm{Tr}\{\rho[\tilde{c}_{\gamma\mathbf{k}}(t),\tilde{d}_\sigma^\dagger(0)]_+\} + \frac{i}{\hbar}\theta(t)\,\mathrm{Tr}\{\rho[\frac{\partial}{\partial t}\tilde{c}_{\gamma\mathbf{k}}(t),\tilde{d}_\sigma^\dagger(0)]_+\}. \tag{5.17}$$

De acordo com a equação de Heisenberg :

$$\frac{\partial}{\partial t}\tilde{c}_{\gamma\mathbf{k}}(t) \;=\; -\frac{i}{\hbar}[\tilde{c}_{\gamma\mathbf{k}}, \mathcal{H}_{\text{Full}}] = -\frac{i}{\hbar}(\tilde{\varepsilon}_{\mathbf{k}}\tilde{c}_{\mathbf{k},\gamma} + \mathcal{V}\tilde{d}_\gamma), \tag{5.18}$$

que produz

---

[1] Por simplicidade, adotamos $\eta \equiv \eta_\uparrow$.

[2] $\tilde{\mathcal{G}}_{\tilde{d}_\sigma,\tilde{d}_{\tilde{\sigma}}}(\varepsilon) = \int dt\, \mathcal{G}_{\tilde{d}_\sigma,\tilde{d}_{\tilde{\sigma}}}(t)e^{\frac{i}{\hbar}\varepsilon t}$

$$i\hbar\frac{\partial}{\partial t}\mathcal{G}_{\tilde{c}_{\gamma k},\tilde{d}_\sigma}(t) = \delta(t)\operatorname{Tr}\{\rho[\tilde{c}_{\gamma k}(t),\tilde{d}_\sigma^\dagger(0)]_+\} + \tilde{\varepsilon}_{\mathbf{k}}(-\frac{i}{\hbar})\theta(t)\operatorname{Tr}\{\rho[\tilde{c}_{\mathbf{k},\gamma}(t),\tilde{d}_\sigma^\dagger(0)]_+\}$$
$$+ \mathcal{V}(-\frac{i}{\hbar})\theta(t)\operatorname{Tr}\{\rho[\tilde{d}_\gamma(t),\tilde{d}_\sigma^\dagger(0)]_+\}. \tag{5.19}$$

Usando a definição da função de Green retardada e realizando a transformada de Fourier na última equação, como realizado na Eq.(5.14), obtemos:

$$\tilde{\mathcal{G}}_{\tilde{c}_{\gamma\mathbf{k}},\tilde{d}_\sigma}(\varepsilon) = \frac{\mathcal{V}}{\varepsilon - \tilde{\varepsilon}_{\mathbf{k}}}\tilde{\mathcal{G}}_{\tilde{d}_\gamma,\tilde{d}_\sigma}(\varepsilon). \tag{5.20}$$

Deste modo, substituindo a Eq.(5.20) na Eq.(5.15), encontramos a relação a seguir:

$$\left(\varepsilon - \varepsilon_{d,\gamma} - \sum_{\mathbf{k}}\frac{|\mathcal{V}|^2}{\varepsilon - \tilde{\varepsilon}_{\mathbf{k}}}\right)\tilde{\mathcal{G}}_{\tilde{d}_\gamma,\tilde{d}_\sigma}(\varepsilon) = \delta_{\sigma\gamma} - \bar{\lambda}_\gamma\tilde{\mathcal{G}}_{\eta,\tilde{d}_\sigma}(\varepsilon) - \bar{\lambda}_\gamma\tilde{\mathcal{G}}_{\eta^\dagger,\tilde{d}_\sigma}(\varepsilon). \tag{5.21}$$

Como se pode ver no lado direito de Eq.(5.21), devemos calcular duas novas funções de Green no domínio da energia, começando com $\tilde{\mathcal{G}}_{\eta,\tilde{d}_\sigma}(\varepsilon)$, definida assim:

$$\mathcal{G}_{\eta,\tilde{d}_\sigma}(t) = -\frac{i}{\hbar}\theta(t)\operatorname{Tr}\{\rho[\eta(t),\tilde{d}_\sigma^\dagger(0)]_+\}. \tag{5.22}$$

Ao derivar tal função de Green no tempo, obtemos

$$i\hbar\frac{\partial}{\partial t}\mathcal{G}_{\eta,\tilde{d}_\sigma}(t) = \delta(t)\operatorname{Tr}\{\rho[\eta(t),\tilde{d}_\sigma^\dagger(0)]_+\} + \theta(t)\operatorname{Tr}\{\rho[\frac{\partial}{\partial t}\eta(t),\tilde{d}_\sigma^\dagger(0)]_+\} \tag{5.23}$$

e de acordo com a equação de Heisenberg:

$$\frac{\partial}{\partial t}\eta(t) = -\frac{i}{\hbar}(\varepsilon_{\mathrm{M}}\eta - \sum_\sigma\bar{\lambda}_\sigma\tilde{d}_\sigma + \sum_\sigma\bar{\lambda}_\sigma\tilde{d}_\sigma^\dagger). \tag{5.24}$$

Substituindo a Eq.(5.24) na Eq.(5.23) e realizando a transformada de Fourier, obtemos a função de Green no domínio da energia que segue:

$$(\varepsilon - \varepsilon_{\mathrm{M}})\tilde{\mathcal{G}}_{\eta,\tilde{d}_\sigma}(\varepsilon) = -\sum_\gamma\bar{\lambda}_\gamma\tilde{\mathcal{G}}_{\tilde{d}_\gamma,\tilde{d}_\sigma}(\varepsilon) + \sum_\gamma\bar{\lambda}_\gamma\tilde{\mathcal{G}}_{\tilde{d}_\gamma^\dagger,\tilde{d}_\sigma}(\varepsilon). \tag{5.25}$$

Do mesmo modo encontramos $\tilde{\mathcal{G}}_{\eta^\dagger,\tilde{d}_\sigma}(\varepsilon)$, dada pela expressão seguinte:

$$(\varepsilon + \varepsilon_{\mathrm{M}})\tilde{\mathcal{G}}_{\eta^\dagger,\tilde{d}_\sigma}(\varepsilon) \quad = \quad -\sum_\gamma \bar{\lambda}_\gamma \tilde{\mathcal{G}}_{\tilde{d}_\gamma,\tilde{d}_\sigma}(\varepsilon) + \sum_\gamma \bar{\lambda}_\gamma \tilde{\mathcal{G}}_{\tilde{d}_\gamma^\dagger,\tilde{d}_\sigma}(\varepsilon). \tag{5.26}$$

Notamos que nas Eqs.(5.25) e (5.26) devemos calcular $\tilde{\mathcal{G}}_{\tilde{d}_\gamma^\dagger,\tilde{d}_\sigma}(\varepsilon)$, a qual é determinada em t como:

$$\mathcal{G}_{\tilde{d}_\gamma^\dagger,\tilde{d}_\sigma}(t) = -\frac{i}{\hbar}\theta(t)\,\mathrm{Tr}\{\rho[\tilde{d}_\gamma^\dagger(t),\tilde{d}_\sigma^\dagger(0)]_+\}, \tag{5.27}$$

que derivando fornece:

$$i\hbar\frac{\partial}{\partial t}\mathcal{G}_{\tilde{d}_\gamma^\dagger,\tilde{d}_\sigma}(t) \quad = \quad \delta(t)\,\mathrm{Tr}\{\rho[\tilde{d}_\gamma^\dagger(t),\tilde{d}_\sigma^\dagger(0)]_+\} + \theta(t)\mathrm{Tr}\{\rho[\frac{\partial}{\partial t}\tilde{d}_\gamma^\dagger(t),\tilde{d}_\sigma^\dagger(0)]_+\}. \tag{5.28}$$

Usando Heisenberg, temos:

$$\frac{\partial}{\partial t}\tilde{d}_\gamma^\dagger(t) \quad = \quad -\frac{i}{\hbar}(-\varepsilon_{d,\gamma}\tilde{d}_\gamma^\dagger - \mathcal{V}\sum_{\mathbf{k}}\tilde{c}_{\gamma\mathbf{k}}^\dagger + \bar{\lambda}_\gamma\eta^\dagger + \bar{\lambda}_\gamma\eta). \tag{5.29}$$

Assim, Eq.(5.28) torna-se:

$$\begin{aligned} i\hbar\frac{\partial}{\partial t}\mathcal{G}_{\tilde{d}_\gamma^\dagger,\tilde{d}_\sigma}(t) \quad = \quad & \delta(t)\,\mathrm{Tr}\{\rho[\tilde{d}_\gamma^\dagger(t),\tilde{d}_\sigma^\dagger(0)]_+\} - \varepsilon_{d,\gamma}(-\frac{i}{\hbar})\theta(t)\,\mathrm{Tr}\{\rho[\tilde{d}_\gamma^\dagger(t),\tilde{d}_\sigma^\dagger(0)]_+\} \\ & -\quad \mathcal{V}\sum_{\mathbf{k}}(-\frac{i}{\hbar})\theta(t)\,\mathrm{Tr}\{\rho[\tilde{c}_{\gamma\mathbf{k}}^\dagger(t),\tilde{d}_\sigma^\dagger(0)]_+\} + \bar{\lambda}_\gamma(-\frac{i}{\hbar})\theta(t)\,\mathrm{Tr}\{\rho[\eta^\dagger(t),\tilde{d}_\sigma^\dagger(0)]_+\} \\ & +\quad \bar{\lambda}_\gamma(-\frac{i}{\hbar})\theta(t)\,\mathrm{Tr}\{\rho[\eta(t),\tilde{d}_\sigma^\dagger(0)]_+\}. \end{aligned} \tag{5.30}$$

De acordo com definição da função de Green retardada, a expressão acima pode ser escrita como:

$$\begin{aligned} i\hbar\frac{\partial}{\partial t}\mathcal{G}_{\tilde{d}_\gamma^\dagger,\tilde{d}_\sigma}(t) \quad = \quad & \delta(t)\,\mathrm{Tr}\{\rho[\tilde{d}_\gamma^\dagger(t),\tilde{d}_\sigma^\dagger(0)]_+\} - \varepsilon_{d,\gamma}\mathcal{G}_{\tilde{d}_\gamma^\dagger,\tilde{d}_\sigma}(t) - \mathcal{V}\sum_{\mathbf{k}}\mathcal{G}_{\tilde{c}_{\gamma\mathbf{k}}^\dagger,\tilde{d}_\sigma}(t) \\ & +\quad \bar{\lambda}_\gamma\mathcal{G}_{\eta^\dagger,\tilde{d}_\sigma}(t) + \bar{\lambda}_\gamma\mathcal{G}_{\eta,\tilde{d}_\sigma}(t). \end{aligned} \tag{5.31}$$

Empregando a transformada de Fourier na Eq.(5.31), obtemos:

$$(\varepsilon + \varepsilon_{d,\gamma})\tilde{\mathcal{G}}_{\tilde{d}_\gamma^\dagger,\tilde{d}_\sigma}(\varepsilon) \quad = \quad -\mathcal{V}\sum_{\mathbf{k}}\tilde{\mathcal{G}}_{\tilde{c}_{\gamma\mathbf{k}}^\dagger,\tilde{d}_\sigma}(\varepsilon) + \bar{\lambda}_\gamma\tilde{\mathcal{G}}_{\eta^\dagger,\tilde{d}_\sigma}(\varepsilon) + \bar{\lambda}_\gamma\tilde{\mathcal{G}}_{\eta,\tilde{d}_\sigma}(\varepsilon). \tag{5.32}$$

Novamente, uma nova função de Green emerge, que é encontrada pelo mesmo procedimento adotado até agora, resultando em:

$$\tilde{\mathcal{G}}_{\tilde{c}_{\gamma k}^{\dagger},\tilde{d}_{\sigma}}\left(\varepsilon\right) \;\; = \;\; -\frac{\mathcal{V}}{\varepsilon+\tilde{\varepsilon}_{\mathbf{k}}}\tilde{\mathcal{G}}_{\tilde{d}_{\gamma}^{\dagger},\tilde{d}_{\sigma}}\left(\varepsilon\right), \tag{5.33}$$

que é substituído na Eq.(5.32), dando origem à seguinte equação:

$$\left(\varepsilon+\varepsilon_{d,\gamma}-\sum_{\mathbf{k}}\frac{|\mathcal{V}|^{2}}{\varepsilon+\tilde{\varepsilon}_{\mathbf{k}}}\right)\tilde{\mathcal{G}}_{\tilde{d}_{\gamma}^{\dagger},\tilde{d}_{\sigma}}\left(\varepsilon\right) \;\; = \;\; \bar{\lambda}_{\gamma}\tilde{\mathcal{G}}_{\eta^{\dagger},\tilde{d}_{\sigma}}\left(\varepsilon\right)+\bar{\lambda}_{\gamma}\tilde{\mathcal{G}}_{\eta,\tilde{d}_{\sigma}}\left(\varepsilon\right). \tag{5.34}$$

Agora, vamos combinar as Eqs.(5.25) e (5.26) nas Eqs. (5.21) e (5.34):

$$\begin{aligned}
(\varepsilon-\epsilon_{d,\gamma}+i\Gamma)\tilde{\mathcal{G}}_{\tilde{d}_{\gamma},\tilde{d}_{\sigma}}\left(\varepsilon\right) \;\; = \;\; & \delta_{\sigma\gamma}+\bar{\lambda}_{\gamma}\sum_{\tilde{\gamma}}\bar{\lambda}_{\tilde{\gamma}}\left(\frac{1}{\varepsilon-\varepsilon_{\mathrm{M}}}+\frac{1}{\varepsilon+\varepsilon_{\mathrm{M}}}\right)\tilde{\mathcal{G}}_{\tilde{d}_{\tilde{\gamma}},\tilde{d}_{\sigma}}\left(\varepsilon\right) \\
& -\bar{\lambda}_{\gamma}\sum_{\tilde{\gamma}}\bar{\lambda}_{\tilde{\gamma}}\left(\frac{1}{\varepsilon+\varepsilon_{\mathrm{M}}}+\frac{1}{\varepsilon-\varepsilon_{\mathrm{M}}}\right)\tilde{\mathcal{G}}_{\tilde{d}_{\tilde{\gamma}}^{\dagger},\tilde{d}_{\sigma}}\left(\varepsilon\right),
\end{aligned} \tag{5.35}$$

onde reconhecemos $\sum_{\mathbf{k}}\frac{|\mathcal{V}|^{2}}{(\varepsilon-\tilde{\varepsilon}_{\mathbf{k}})}\equiv-i\pi V^{2}\sum_{\mathbf{k}}\delta(\varepsilon-\varepsilon_{\mathbf{k}})=-i\Gamma$ como parâmetro de Anderson [34] e $K=\left(\frac{1}{\varepsilon-\varepsilon_{\mathrm{M}}}+\frac{1}{\varepsilon+\varepsilon_{\mathrm{M}}}\right)$. Assim,

$$\begin{aligned}
(\varepsilon-\varepsilon_{d,\gamma}+i\Gamma)\tilde{\mathcal{G}}_{\tilde{d}_{\gamma},\tilde{d}_{\sigma}}\left(\varepsilon\right) \;\; = \;\; & \delta_{\sigma\gamma}+\bar{\lambda}_{\gamma}K\left[\bar{\lambda}_{\uparrow}\tilde{\mathcal{G}}_{\tilde{d}_{\uparrow},\tilde{d}_{\sigma}}\left(\varepsilon\right)+\bar{\lambda}_{\downarrow}\tilde{\mathcal{G}}_{\tilde{d}_{\downarrow},\tilde{d}_{\sigma}}\left(\varepsilon\right)\right] \\
& -\bar{\lambda}_{\gamma}K\left[\bar{\lambda}_{\uparrow}\tilde{\mathcal{G}}_{\tilde{d}_{\uparrow}^{\dagger},\tilde{d}_{\sigma}}\left(\varepsilon\right)+\bar{\lambda}_{\downarrow}\tilde{\mathcal{G}}_{\tilde{d}_{\downarrow}^{\dagger},\tilde{d}_{\sigma}}\left(\varepsilon\right)\right]
\end{aligned} \tag{5.36}$$

e similarmente encontramos:

$$(\varepsilon+\varepsilon_{d,\gamma}+i\Gamma)\tilde{\mathcal{G}}_{\tilde{d}_{\gamma}^{\dagger},\tilde{d}_{\sigma}}\left(\varepsilon\right) \;\; = \;\; -\bar{\lambda}_{\gamma}K\sum_{\tilde{\gamma}}\bar{\lambda}_{\tilde{\gamma}}\tilde{\mathcal{G}}_{\tilde{d}_{\tilde{\gamma}},\tilde{d}_{\sigma}}\left(\varepsilon\right)+\bar{\lambda}_{\gamma}K\sum_{\tilde{\gamma}}\bar{\lambda}_{\tilde{\gamma}}\tilde{\mathcal{G}}_{\tilde{d}_{\tilde{\gamma}}^{\dagger},\tilde{d}_{\sigma}}\left(\varepsilon\right). \tag{5.37}$$

Finalmente, as Eqs.(5.36) e (5.37), temos um sistema de funções de Green mapeado no *pseudospin*:

$$\begin{aligned}
(\varepsilon-\epsilon_{d\sigma}-\bar{\lambda}_{\sigma}^{2}K+i\Gamma)\tilde{\mathcal{G}}_{\tilde{d}_{\sigma},\tilde{d}_{\sigma}}-\bar{\lambda}_{\bar{\sigma}}\bar{\lambda}_{\sigma}K\tilde{\mathcal{G}}_{\tilde{d}_{\bar{\sigma}},\tilde{d}_{\sigma}} & \\
+\bar{\lambda}_{\sigma}^{2}K\tilde{\mathcal{G}}_{\tilde{d}_{\sigma}^{\dagger},\tilde{d}_{\sigma}}+\bar{\lambda}_{\sigma}\bar{\lambda}_{\bar{\sigma}}K\tilde{\mathcal{G}}_{\tilde{d}_{\bar{\sigma}}^{\dagger},\tilde{d}_{\sigma}} & =1,
\end{aligned} \tag{5.38}$$

$$\begin{aligned}
-\bar{\lambda}_{\sigma}\bar{\lambda}_{\bar{\sigma}}K\tilde{\mathcal{G}}_{\tilde{d}_{\bar{\sigma}},\tilde{d}_{\bar{\sigma}}}+(\varepsilon-\epsilon_{d\sigma}-\bar{\lambda}_{\sigma}^{2}K+i\Gamma)\tilde{\mathcal{G}}_{\tilde{d}_{\sigma},\tilde{d}_{\bar{\sigma}}} & \\
+\bar{\lambda}_{\sigma}\bar{\lambda}_{\bar{\sigma}}K\tilde{\mathcal{G}}_{\tilde{d}_{\bar{\sigma}}^{\dagger},\tilde{d}_{\bar{\sigma}}}+\bar{\lambda}_{\sigma}^{2}K\tilde{\mathcal{G}}_{\tilde{d}_{\sigma}^{\dagger},\tilde{d}_{\bar{\sigma}}} & =0,
\end{aligned} \tag{5.39}$$

$$\bar{\lambda}_\sigma^2 K \tilde{\mathcal{G}}_{\tilde{d}_\sigma,\tilde{d}_\sigma} + \bar{\lambda}_\sigma \bar{\lambda}_{\bar{\sigma}} K \tilde{\mathcal{G}}_{\tilde{d}_{\bar{\sigma}},\tilde{d}_\sigma}$$

$$+(\varepsilon + \epsilon_{d\sigma} - \bar{\lambda}_\sigma^2 K + i\Gamma)\tilde{\mathcal{G}}_{\tilde{d}_\sigma^\dagger,\tilde{d}_\sigma} - \bar{\lambda}_\sigma \bar{\lambda}_{\bar{\sigma}} K \tilde{\mathcal{G}}_{\tilde{d}_{\bar{\sigma}}^\dagger,\tilde{d}_\sigma} = 0 \qquad (5.40)$$

e

$$\bar{\lambda}_\sigma \bar{\lambda}_{\bar{\sigma}} K \tilde{\mathcal{G}}_{\tilde{d}_{\bar{\sigma}},\tilde{d}_{\bar{\sigma}}} + \bar{\lambda}_\sigma^2 K \tilde{\mathcal{G}}_{\tilde{d}_\sigma,\tilde{d}_{\bar{\sigma}}} - \bar{\lambda}_{\bar{\sigma}} \bar{\lambda}_\sigma K \widetilde{\mathcal{G}}_{\tilde{d}_{\bar{\sigma}}^\dagger,\tilde{d}_{\bar{\sigma}}}$$

$$+(\varepsilon + \epsilon_{d\sigma} - \bar{\lambda}_\sigma^2 K + i\Gamma)\tilde{\mathcal{G}}_{\tilde{d}_\sigma^\dagger,\tilde{d}_{\bar{\sigma}}} = 0, \qquad (5.41)$$

onde $\bar{\sigma}$ é o oposto de σ. Para realizar a análise do modelo na próxima seção, informamos que resolvemos o sistema acima numericamente.

Capítulo 6

Resultados e Discussão

Nas simulações abaixo a temperatura é $T = 0$ e $\Gamma = 40\mu eV$[8, 34]. A cadeia topológica de Kitaev, por uma questão de simplicidade, é tratada como muito grande, o que impõe $\varepsilon_M \rightarrow 0$. Assim, a fim de tornar explícito o fenômeno da criptografia do *qubit*, começamos a discutir o cenário solicitado para os resultados da Fig.6.1. A Fig.6.1 (a) considera $\varepsilon_R = -2\Gamma$, $|\lambda_L| = |\lambda_R| = \lambda = 5\Gamma$, $T_c = 1\Gamma$ e $\varepsilon_L = 1\Gamma$, onde verificamos um ZBP com amplitude de $1/4$ na $\mathcal{T}_{\text{Total}}$ da Eq.(5.5) como uma função de ε. Esta ressonância detectável representa o vazamento do *qubit* $\eta_\uparrow$ para a configuração de dois QDs. Além disso, ele também representa o registro do *qubit* decriptado sobre o QD esquerdo, que será posteriormente elucidado através da Fig.6.1. Neste ponto, consideremos a sequência de painéis de (b) até (d), que descreve a criptografia em si: mudando apenas ε_L, percebemos que a amplitude do ZBP começa a reduzir-se progressivamente até a extinção total na Fig.6.1(d). Neste caso, apenas um par de picos permanece visível denotando o hiato *pseudo*-Zeeman renormalizado $\tilde{\epsilon}_{d\uparrow} - \tilde{\epsilon}_{d\downarrow}$. Na verdade, vamos esclarecer que o ZBP torna-se BICs, sendo indetectável por $\mathcal{T}_{\text{Total}}$. Isso significa que, se o ZBP não for percebido, temos a realização da criptografia do *qubit*, que aparece abordada em detalhes pelas Figs.6.2 and 6.3.

A Fig.6.2 exibe os *density plots* das contribuições parciais $\mathcal{T}_{\text{Total}}$, $\mathcal{T}_{LL}$ e $\mathcal{T}_{RR}$ nos eixos ε e ε_L para $\varepsilon_R = -2\Gamma$ ($\varepsilon_R = -1.5\Gamma$), $\lambda = 5\Gamma$ ($|\lambda_L| = 1.95\Gamma$ e $|\lambda_R| = 5\Gamma$) e $T_c = 1\Gamma$. Vale a pena notar que todos os painéis nas Figs.6.2(a)-(f) apresentam uma estrutura ZBP. No entanto, cada um revela aspectos diferentes do efeito de vazamento. Por exemplo, na Fig.6.2(a)((d)) destacamos a região superior marcada por uma elipse amarela tracejada: vê-se o domínio onde a criptografia do *qubit* é permitida, uma vez que o ZBP está ausente. As Figs.6.2(b)((e)) e (c)((f)) contêm o vazamento assimétrico nos QDs e a decriptografia do *qubit* aparecendo à esquerda. Observe que próximo de $\varepsilon_L = 1\Gamma$ ($\varepsilon_L = 0$), o QD da direita desacopla da configuração, devido à $\mathcal{T}_{RR} = 0$. Esta região é então identificada por elipses brancas tracejadas nos painéis (a)-(f) da mesma figura. Como resultado, o *qubit* é registrado unicamente no QD esquerdo como a Fig.6.2(b)((e)) assegura. Isso corresponde à leitura do *qubit* dada pela medição de carga como proposto por Flensberg [33]. Observe que $\mathcal{T}_{LL}$ e $\mathcal{T}_{RR}$ compartilham o mesmo brilho em suas escalas, ressaltando que o vazamento simétrico do modo zero do *qubit* é robusto diante de acoplamentos assimétricos. No que diz respeito aos picos satélites nas Figs.6.2(a)-(f), eles delimitam o hiato *pseudo*-Zeeman renormalizado $\tilde{\epsilon}_{d\uparrow} - \tilde{\epsilon}_{d\downarrow}$. Esses picos estão predominantemente ausentes, como podemos ver,
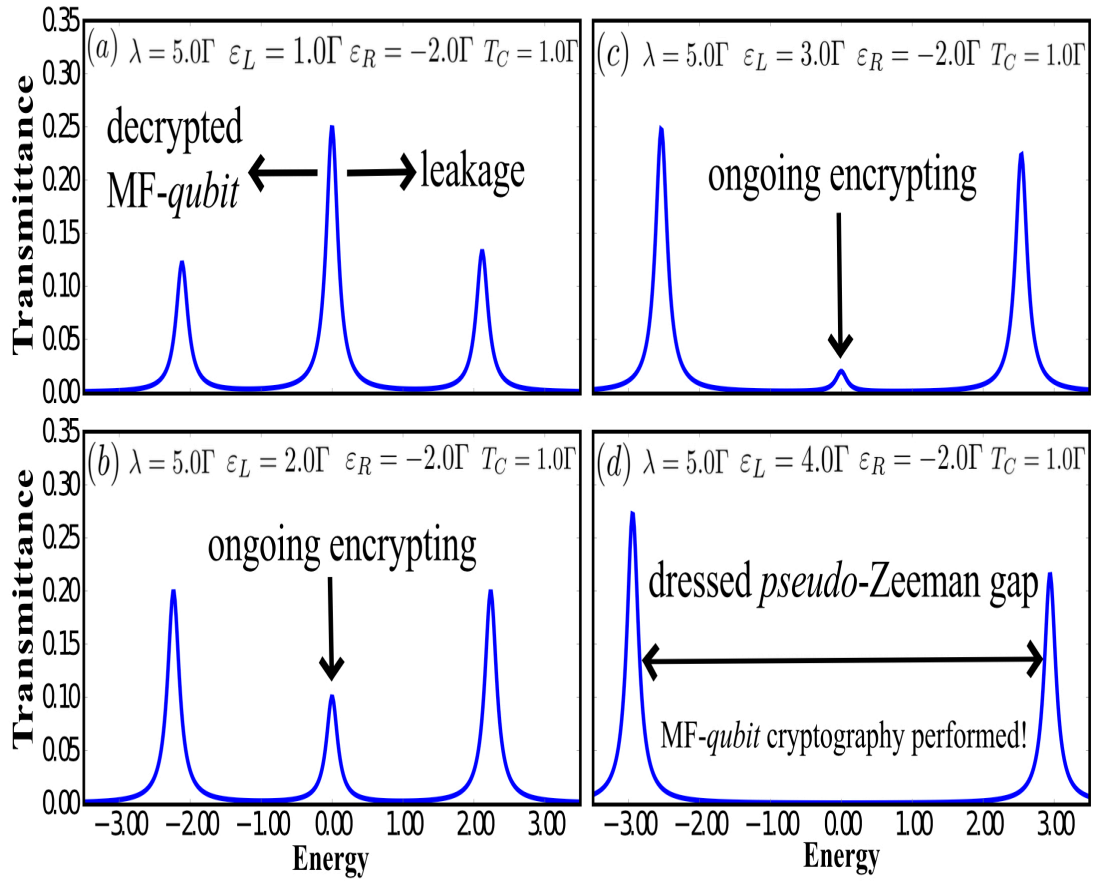
Figura 6.1: $\mathcal{T}_{\text{Total}}$ como uma função de ε: (a) O ZBP fornece o vazamento assimétrico do *qubit* $\eta_\uparrow$ no QD da esquerda (veja também a Fig.6.2. (b)-(c)). O aumento do ε_R produz o processo para criptografar este *qubit*, que é caracterizado pela extinção da amplitude do ZBP. (d) Aqui o ZBP (o *qubit*) está escondido como BICs igualmente divididos nos QDs, onde apenas o hiato pseudo-Zeeman renormalizado é visível (veja também Fig.6.3).

na região inferior de Fig.6.2(a). Este ponto implica em BICs fora do ZBP. Por isso, para entender completamente a física subjacente no aparecimento da decriptografia do *qubit* no QD da esquerda versus a criptografia em si, devemos considerar a Fig.6.3, que usa os mesmos parâmetros da Fig.6.1 apenas por uma questão de escolha, uma vez que para o surgimento dos BICs, o vazamento é sempre simétrico, mesmo com acoplamentos assimétricos λ_L e λ_R como as Figs.6.2(e) e (f) asseguram.

Na Fig. 6.3 (a) a análise de $\mathcal{T}_{jl}$ mostra que o vazamento do MF ocorre apenas no QD da esquerda. Desta forma, a situação de *qubit* decriptado é alcançada: $\mathcal{T}_{LL}$ exibe um ZBP com amplitude $1/4$ em contraste com $\mathcal{T}_{RR}$. Assim, para entender esse problema, devemos focar nos *insets*. $\mathcal{T}_{RR}$ apresenta $\mathcal{T}_{\uparrow\uparrow} + \mathcal{T}_{\downarrow\downarrow}$ perfeitamente deslocado de π em relação à $\mathcal{T}_{\uparrow\downarrow} + \mathcal{T}_{\downarrow\uparrow}$ (antirressonância Fano) [39, 40], portanto resultando em um QD desacoplado da configuração. Para $\mathcal{T}_{LL}$, $\mathcal{T}_{\uparrow\uparrow} + \mathcal{T}_{\downarrow\downarrow}$ e $\mathcal{T}_{\uparrow\downarrow} + \mathcal{T}_{\downarrow\uparrow}$ se interferem construtivamente. Na Fig.6.3(b) para $\mathcal{T}_{RR}$, a antirressonância Fano $\mathcal{T}_{\uparrow\downarrow} + \mathcal{T}_{\downarrow\uparrow}$ não é perfeita como anteriormente e não cancela mais $\mathcal{T}_{\uparrow\uparrow} + \mathcal{T}_{\downarrow\downarrow}$. Particularmente, a antirressonância Fano encontrada em $\mathcal{T}_{LR} + \mathcal{T}_{RL}$ interfere destrutivamente e perfeitamente com o pico em $\mathcal{T}_{LL} + \mathcal{T}_{RR}$. Deste modo, a criptografia do *qubit* é garantida nos dois QDs, o qual está escondido como BICs, os quais estão igualmente divididos nesses QDs com amplitude $1/8$ cada. Estes processos aparecem esboçados na região inferior das Figs. 6.3(a) and (b).
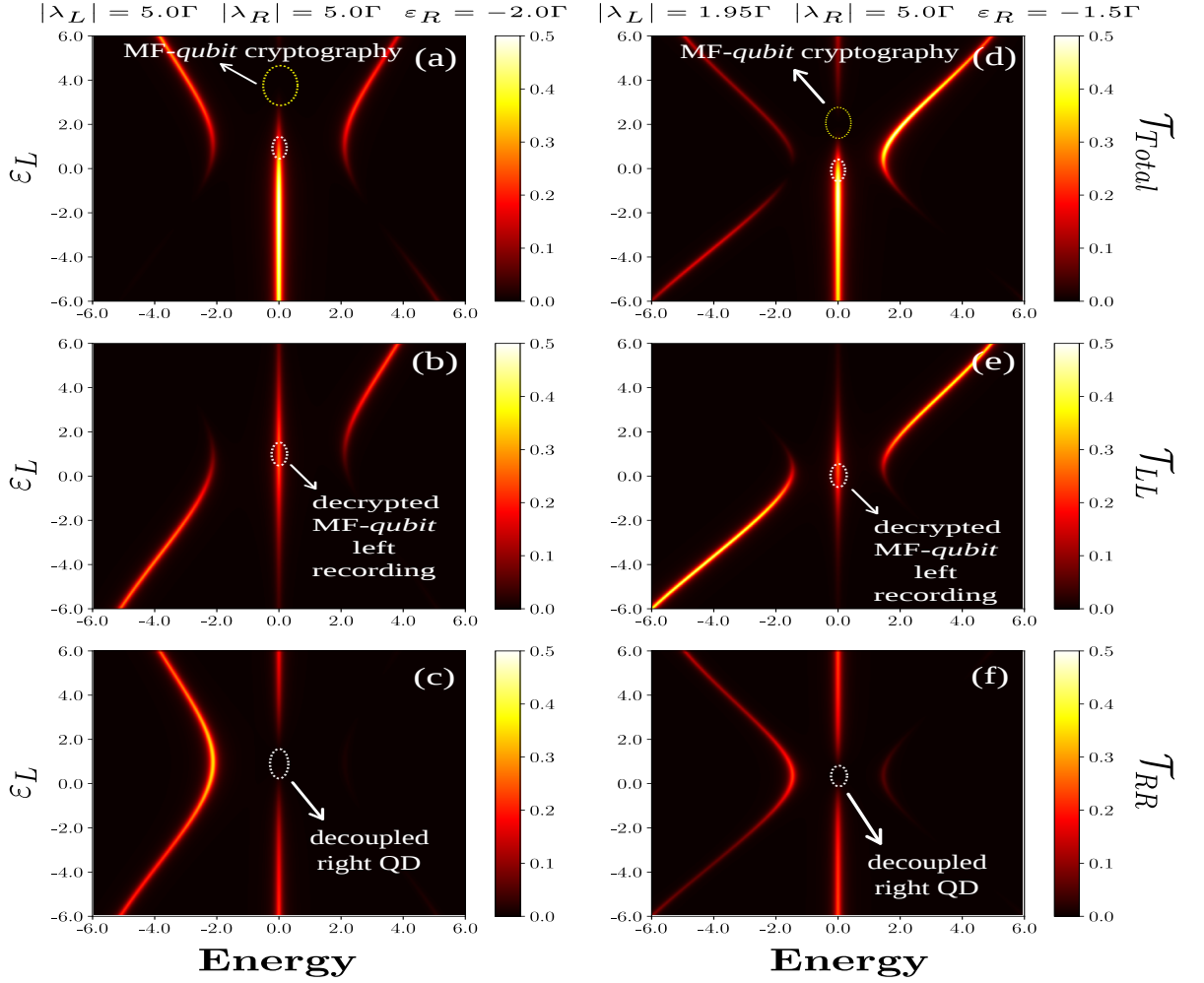
31

Figura 6.2: Parcelas das densidades de transmitância: (a) $\mathcal{T}_{\text{Total}}$, (b) $\mathcal{T}_{LL}$ e (c) $\mathcal{T}_{RR}$ nos eixos ε_L e ε, com $\varepsilon_R = -2\Gamma$, $|\lambda_L| = |\lambda_R| = \lambda = 5\Gamma$ e $T_c = 1\Gamma$. As elipses retratadas mostram o ZBP: i) a região para a criptografia do *qubit* (elipse amarela tracejada) em (a) e ii) O correspondente para o registro/aparecimento do *qubit* decriptado na esquerda (elipse branca tracejada a) em (a) e (b), devido o QD da direita estar totalmente desacoplado do sistema como o painel (c) mostra (elipse branca tracejada). Painéis (d),(e) e (f) para $|\lambda_L| \neq |\lambda_R|$ dão qualitativamente o mesmo de (a), (b) e (c) garantindo assim a robusteza topológica dos resultados, ou seja, os BICs (o *qubit* encriptado) e o *qubit* decriptado registrado na esquerda ainda ocorrem, mas para diferentes conjuntos de parâmetros.
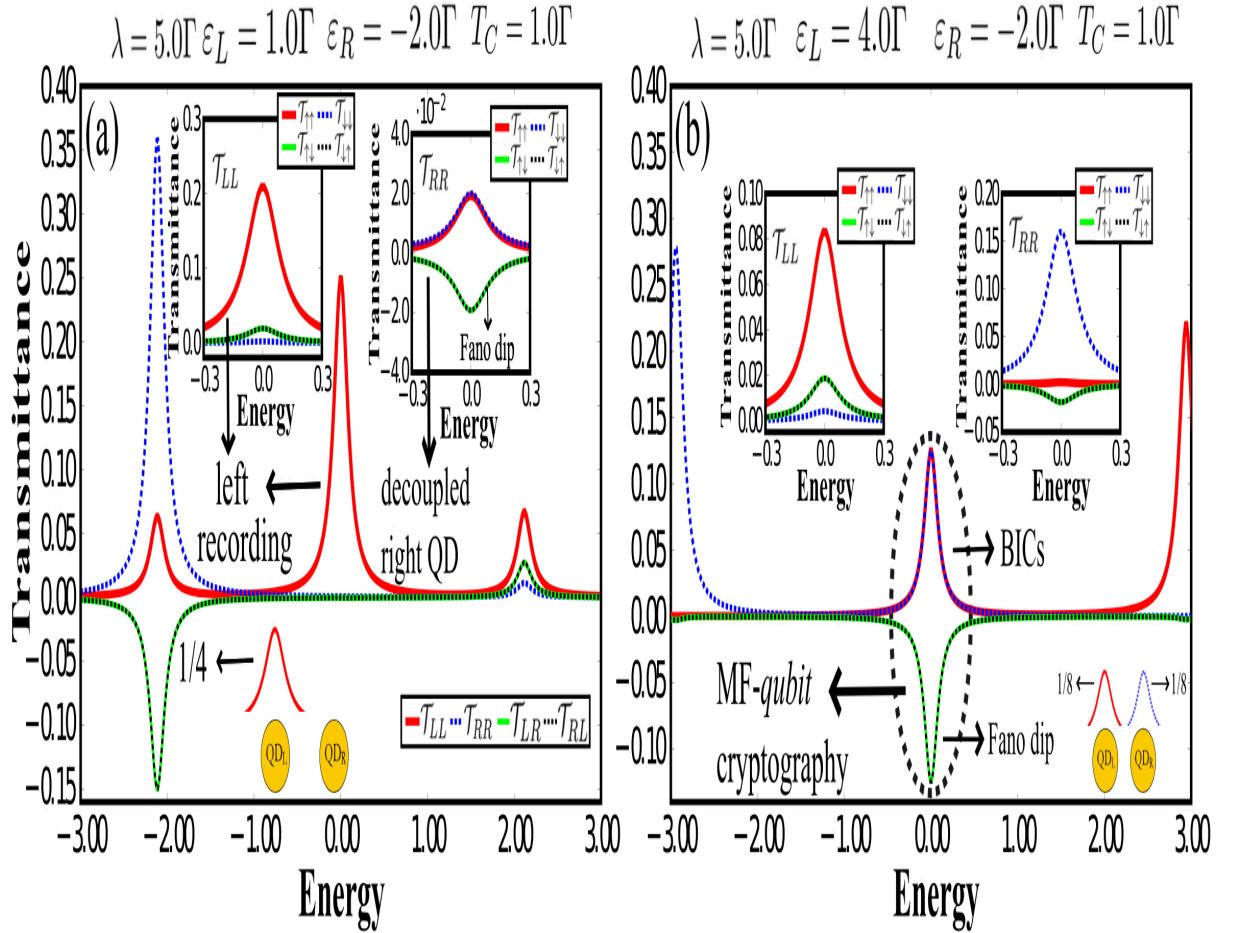
Figura 6.3: $\mathcal{T}_{jl}$ em (a) caracterizando o aparecimento do *qubit* decriptado na esquerda. $\mathcal{T}_{LL}$ mostra o ZBP com amplitude de $1/4$, enquanto no $\mathcal{T}_{RR}$ ele não existe: o inset revela que o $\mathcal{T}_{RR}$ exibe $\mathcal{T}_{\uparrow\uparrow} + \mathcal{T}_{\downarrow\downarrow}$ fase perfeitamente deslocado de π com respeito à $\mathcal{T}_{\uparrow\downarrow} + \mathcal{T}_{\downarrow\uparrow}$ (antirressonância Fano). Como consequência, este QD é desacoplado do sistema. Em (b), temos a criptografia do *qubit*: em $\mathcal{T}_{RR}$, a antirressonância Fano não é perfeita como antes. Contudo, a antirressonância Fano em $\mathcal{T}_{LR} + \mathcal{T}_{RL}$ interfere destrutivamente e exatamente com $\mathcal{T}_{LL} + \mathcal{T}_{RR}$. Isso significa que o *qubit* está escondido como BICs igualmente divididos nos QDs.

Capítulo 7

Conclusões

Em resumo, encontramos teoricamente que a criptografia do *qubit* de MFs é viável no sistema da Fig. 1.1(a). Mostramos que o *qubit* decriptado ocorre em um único QD devido a um vazamento assimétrico do estado de MF nos QDs. O *qubit* encriptado ocorre quando o vazamento é simétrico, onde o estado vazado do *qubit* está na forma de BICs. Assim, propomos um mecanismo de leitura do *qubit* $\eta_\uparrow = \frac{1}{\sqrt{2}}(\Psi_1 + i\Psi_2)$ por meio do ZBP que emerge nos QDs, provendo assim, a implementação da criptografia quântica da mensagem escrita nos estados Ψ_1 e Ψ_2 inicialmente preparados nas bordas da cadeia topológica de Kitaev. Portanto, entendemos que nossos resultados podem ser aplicados no contexto da computação quântica topológica. Em anexo, aprentamos o artigo publicado sobre o tema desta dissertação, o qual pode ser encontrado no Physical Review B 96, 041114 (Rapid Communication) (2017).

Referências Bibliográficas

[1] J. Alicea, Rep. Prog. Phys. **75**, 076501 (2012).

[2] S. R. Elliott and M. Franz, Rev. Mod. Phys. **87**, 137 (2015).

[3] A. Y. Kitaev, Phys. Usp. **44**, 131 (2001).

[4] A. A. Zyuzin, D. Rainis, J. Klinovaja, and D. Loss, Phys. Rev. Lett. **111**, 056802 (2013).

[5] D. Rainis, J. Klinovaja, L. Trifunovic, and D. Loss, Phys. Rev. B **87**, 024515 (2013).

[6] A. Zazunov, P. Sodano, and R. Egger, New J. Phys **15**, 035033 (2013).

[7] D. Roy, C. J. Bolech, and N. Shah, Phys. Rev. B **86**, 094503 (2012).

[8] E. Vernek, P. H. Penteado, A. C. Seridonio, and J. C. Egues, Phys. Rev. B **89**, 165314 (2014).

[9] M. T. Deng, S. Vaitiekenas, E. B. Hansen, J. Danon, M. Leijnse, K. Flensberg, J. Nygard, P. Krogstrup, and C. M. Marcus, Science **354**, 6319 (2016).

[10] G. Moore and N. Read, Nucl. Phys. B **360**, 362 (1991).

[11] L. Fu, C. L. Kane, and E. J. Mele, Phys. Rev. Lett. **98**, 106803 (2007).

[12] L. Fu and C.L. Kane, Phys. Rev. Lett. **100**, 096407 (2008).

[13] J. D. Sau, R. M. Lutchyn, S. Tewari, and S. Das Sarma, Phys. Rev. Lett. **104**, 040502 (2010).

[14] T. Kawakami and X. Hu, Phys. Rev. Lett. **115**, 177001 (2015).

[15] S. N.- Perge, I. K. Drozdov, J. Li, H. Chen, S. Jeon, J. Seo, A. H. MacDonald, B. A. Bernevig, and A. Yazdani, Science **346**, 602 (2014).

[16] R. Pawlak, M. Kisiel, J. Klinovaja, T. Meier, S. Kawai, T. Glatzel, D. Loss, and E. Meyer, Nature Partner Journals Quantum Information **2**, 16035 (2016).

[17] V. Mourik, K. Zuo, S. M. Frolov, S. R. Plissard, E. P. A. M. Bakkers, and L. P. Kouwenhoven, Science **336**, 1003 (2012).

[18] J. von Neumann and E. Wigner, Phys. Z. **30**, 465 (1929).

[19] F. H. Stillinger and D. R. Herrick, Phys. Rev. A **11**, 446 (1975).

[20] C. W. Hsu, B. Zhen, A. D. Stone, J. D. Joannopoulos, and M. Soljacic, Nature Review Materials, **1**, 16048 (2016).

[21] L. H. Guessi, Y. Marques, R. S. Machado, L.S. Ricco, K. Kristinsson, M. S. Figueira, I. A. Shelykh, M. de Souza, and A. C. Seridonio, Phys. Rev. B **92**, 245107 (2015).

[22] L. H. Guessi, R. S. Machado, Y. Marques, L. S. Ricco, K. Kristinsson, M. Yoshida, I.A. Shelykh, M. de Souza, and A. C. Seridonio, Phys. Rev. B **92**, 045409 (2015).

[23] W.-J. Gong, X.-Y. Sui, Y. Wang, G.-D. Yu, and X.-H. Chen, Nanoscale Research Letters 8, 330 (2013).

[24] Y. Boretz, G. Ordonez, S. Tanaka, and T. Petrosky, Phys. Rev. A **90**, 023853 (2014).

[25] A. Crespi, L. Sansoni, G. D. Valle, A. Ciamei, R. Ramponi, F. Sciarrino, P. Mataloni, S. Longhi, and R. Osellame, Phys. Rev. Lett. **114**, 090201 (2015).

[26] C. W. Hsu, B. Zhen, J. Lee, S.-L. Chua, S. G. Johnson, J.D. Joannopoulos, and M. Soljačić, Nature **499**, 188 (2013).

[27] Y. Plotnik, O. Peleg, F. Dreisow, M. Heinrich, S. Nolte, A. Szameit, and M. Segev, Phys. Rev. Lett. **107**, 183901 (2011).

[28] J. M.-Petit and R. A. Molina, Phys. Rev. B **90**, 035434 (2014).

[29] G. D. Valle and S. Longhi, Phys. Rev. B **89**, 115118 (2014).

[30] C. González-Santander, P. A. Orellana, and F. Domínguez-Adame, Europhys. Lett. **102**, 17012 (2013).

[31] L. S. Ricco, Y. Marques, F. A. Dessotti, R. S. Machado, M. de Souza, and A. C. Seridonio Phys. Rev. B **93**, 165116 (2016).

[32] F. A. Dessotti, L. S. Ricco, Y. Marques, L. H. Guessi, M. Yoshida, M. S. Figueira, M. de Souza, Pasquale Sodano, and A. C. Seridonio Phys. Rev. B **94**, 125426 (2016).

[33] Karsten Flensberg, Phys. Rev. Lett. **106**, 090503 (2011).

[34] P. W. Anderson, Phys. Rev. **124**, 41 (1961).

[35] H. Haug and A. P. Jauho, Quantum Kinetics in Transport and Optics of Semiconductors, Springer Series in Solid-State Sciences 123 (Springer, New York, 1996).

[36] D. E. Liu and H. U. Baranger, Phys. Rev. B **84**, 201308(R) (2011).

[37] M. Leijnse and K. Flensberg, Phys. Rev. B **84**, 140501(R) (2011).

[38] M. Leijnse and K. Flensberg, Phys. Rev. B **86**, 134528 (2012).

[39] U. Fano, Phys. Rev. **124**, 1866 (1961).

[40] A. E. Miroshnichenko, S. Flach, and Y. S. Kivshar, Rev. Mod. Phys. **82**, 2257 (2010).

Encrypting Majorana Fermions-*qubits* as Bound States in the Continuum

L. H. Guessi[1,2], F. A. Dessotti[3], Y. Marques[3], L. S. Ricco[3],
G. M. Pereira[1], P. Menegasso[1,4], M. de Souza[1], and A. C. Seridonio[1,3]

[1] *IGCE, Unesp - Univ Estadual Paulista, Departamento de Física, 13506-900, Rio Claro, SP, Brazil*
[2] *Instituto de Física de São Carlos, Universidade de São Paulo, C.P. 369, São Carlos, SP, 13560-970, Brazil*
[3] *Departamento de Física e Química, Unesp - Univ Estadual Paulista, 15385-000, Ilha Solteira, SP, Brazil*
[4] *Instituto de Física "Gleb Wataghin", Unicamp, Campinas-SP, 13083-859, Brazil*

We theoretically investigate a topological Kitaev chain connected to a double quantum-dot (QD) setup hybridized with metallic leads. In this system, we observe the emergence of two striking phenomena: i) a decrypted Majorana Fermion (MF)-*qubit* recorded over a single QD, which is detectable by means of conductance measurements due to the asymmetrical MF-leaked state into the QDs; ii) an encrypted *qubit* recorded in both QDs when the leakage is symmetrical. In such a regime, we have a cryptographylike manifestation, since the MF-*qubit* becomes bound states in the continuum, which is not detectable in conductance experiments.

Introduction.—It is well known that Majorana fermions (MFs) zero-modes[1, 2] are expected to appear bounded to the edges of a topological Kitaev chain[3–7]. Interestingly enough, by approaching the Kitaev chain to a quantum dot (QD), the MF state leaks[8] into it and manifests itself as a zero-bias peak (ZBP) in conductance measurements. The latter reveals experimentally the MF-*qubit* recorded over the QD. Indeed, such a phenomenon was experimentally confirmed in a QD hybrid-nanowire made by InAs/Al[9] with huge spin-orbit interaction and magnetic fields, being the nanowire placed close to an *s*-wave superconductor. It is worth mentioning that MFs can also emerge in the fractional quantum Hall state with filling-factor $\nu = 5/2$[10], in three-dimensional topological insulators[11], at the core of superconducting vortices[12–14] and on the edges of ferromagnetic atomic chains covering superconductors with pronounced spin-orbit interaction[15, 16], similarly to semiconducting nanowires[17]. In terms of technological applications, MFs-*qubits* are of particular interest. This is because of their topological protection against decoherence[3], a key ingredient for the achievement of efficient quantum computers.

In this work, we show that the employment of two QDs, as depicted in Fig.1(a), enables the cryptography of the MF-*qubit* state $\eta_\uparrow = \frac{1}{\sqrt{2}} (\Psi_1 + i\Psi_2)$ made by the MFs Ψ_1 and Ψ_2 with splitting energy $\varepsilon_M \to 0$, where an encoded message can be written over these states of bits. Our main theoretical findings rely on the interplay between the leakage effect and the so-called bound states in the continuum (BICs)[18, 19]. In this context, it is worth recalling the underlying Physics of such exotic excitations. BICs were proposed by von Neumann and Wigner in 1929[18] as quantum states with localized square-integrable wave functions, but surprisingly within the domain of the energy continuum region. Noteworthy, such states trap particles indefinitely. BICs constitute a current topic of broad interest[20], appearing in several physical systems like graphene[21–23], optics and photonics[24–27], arrangements exhibiting singular
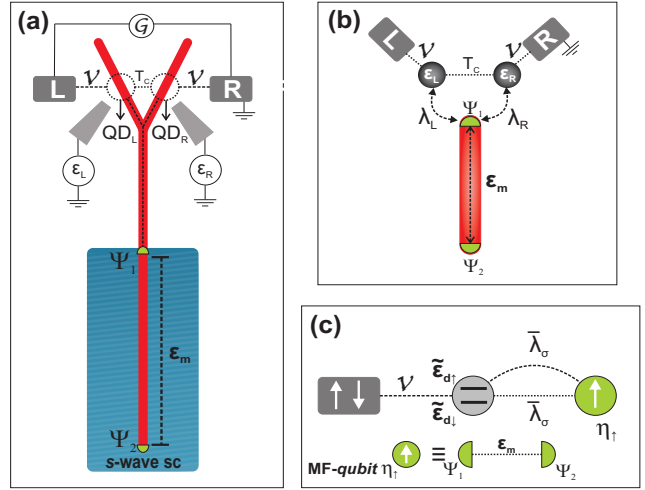

Figure 1. (Color online) (a) Two QDs symmetrically coupled to leads via the hybridization $\mathcal{V}$ and asymmetrically to a topological Kitaev chain by means of the complex amplitudes λ_L and λ_R. Ψ_1 and Ψ_2 are overlapped MFs with splitting energy $\varepsilon_M \to 0$. (b) Oversimplified sketch of panel (a). (c) Mapping of the original system from panel (b) onto the *pseudospin* representation. The dressed *pseudo*-Zeeman gap $\tilde{\epsilon}_{d\uparrow} - \tilde{\epsilon}_{d\downarrow}$ appears depicted within the central QD, which is side-coupled to the *qubit* $\eta_\uparrow$, namely, the MF-*qubit*. $\bar{\lambda}_\sigma$ identifies both the tunneling and the Cooper pair binding energy between the new QD and $\eta_\uparrow$, respectively given by the horizontal and semi-circular dashed lines.

chirality[28] and Floquet-Hubbard states due to A.C. fields[29, 30]. Moreover, BICs assisted by MFs enable applications like the storage of *qubits*[31] and the electrical current switch[32] as well. It should be mentioned that electrons trapped at BICs are prevented to decay into the energy continuum of the environment. Once BICs are undetectable by electrical conductance and accounting for the leakage effect, we benefit of such a remarkable invisibility feature of the BICs. Hence, for the sake of simplicity, we label by cryptography of the MF-

---

qubit $\eta_\uparrow = \frac{1}{\sqrt{2}}(\Psi_1 + i\Psi_2)$ when its ZBP signature disappears as a BIC, turning itself undetectable via conductance measurements. As it will be discussed below, we also find an asymmetrical leakage of the MF-*qubit*. In such a situation, the ZBP is visible in the conductance and we call such a regime by decrypted MF-*qubit*, since the MF state from the Kitaev chain edge leaks solely into a single QD of the proposed setup (Fig.1). Equivalently, the *qubit* is recorded over this QD. Our decrypted MF case corresponds to the readout of the *qubit* in QDs via charge measurement, i.e, the ZB-conductance, as proposed by Flensberg[33]. Otherwise, the encrypted *qubit* is achieved when the recording is symmetrical over the QDs, but with an invisible ZBP in the conductance in such a way that the readout is off, i.e., the decrypting is not allowed. In this regime, the MF-leaked state at zerobias is split into the QDs, thus becoming BICs. Thereby, we propose that the switch on/off of the readout of the *qubit* via the ZBP in the QDs consists in a manner of realizing quantum cryptography of the information written in the prepared MFs states Ψ_1 and Ψ_2.

The Model.—Below we describe theoretically the setup outlined in Fig.1(a) with a topological Kitaev chain coupled to a double QD setup hybridized with metallic leads[33, 34]. The oversimplified sketch of such a system is depicted in Fig.1(b), which is ruled by the Hamiltonian

$$\mathcal{H}_{\text{Full}} = \sum_{\alpha\mathbf{k}} \tilde{\varepsilon}_{\alpha\mathbf{k}} c^\dagger_{\alpha\mathbf{k}} c_{\alpha\mathbf{k}} + \sum_\alpha \varepsilon_\alpha d^\dagger_\alpha d_\alpha + T_{\text{c}}(d^\dagger_L d_R + \text{H.c.}) + \mathcal{V}\sum_{\alpha\mathbf{k}}(c^\dagger_{\alpha\mathbf{k}} d_\alpha + \text{H.c.}) + \mathcal{H}_{\text{MFs}}, \tag{1}$$

where the electrons in the lead $\alpha = L, R$ are described by the operator $c^\dagger_{\alpha\mathbf{k}}$ ($c_{\alpha\mathbf{k}}$) for the creation (annihilation) of an electron in a quantum state labeled by the wave number $\mathbf{k}$ and energy $\tilde{\varepsilon}_{\alpha\mathbf{k}} = \tilde{\varepsilon}_{\mathbf{k}} - \mu_\alpha$, with μ_α as the chemical potential. For the QDs coupled to the leads, $d^\dagger_\alpha$ (d_α) creates (annihilates) an electron in the state ε_α, which is gate tunable. The left-right QD coupling is T_{c}, while $\mathcal{V}$ stands for the hybridization between these QDs and the leads. Concerning $\mathcal{H}_{\text{MFs}}$ we refer to Ref.[33] which accounts for QDs with large energy spacing of levels between spins up and down due to Zeeman splitting. Consequently, the spinless condition is fulfilled where only spin up state is relevant for the emerging topological superconductivity. In this way, our QDs do not depend on the charging energy as in Refs.[9,35], thus the QDs just couple asymmetrically to the Kitaev chain with complex tunneling amplitudes λ_L and λ_R, respectively for the left and right QDs as follows

$$\mathcal{H}_{\text{MFs}} = i\varepsilon_M \Psi_1\Psi_2 + |\lambda_R|(e^{i\phi_R} d_R - e^{-i\phi_R} d^\dagger_R)\Psi_1 + |\lambda_L|(e^{i\phi_L} d_L - e^{-i\phi_L} d^\dagger_L)\Psi_1, \tag{2}$$

where $\Psi_1 = \Psi_1^\dagger$ and $\Psi_2 = \Psi_2^\dagger$ account for the MFs lying on the edges of the chain with overlap term $\varepsilon_M \sim e^{-L/\xi}$, wherein L and ξ designate respectively, the size of the Kitaev chain and the superconducting coherence length.

We stress that, for a sake of simplicity, by employing the following substitutions $d_L = e^{-i\phi_L}[(\cos\theta)\tilde{d}_\uparrow - (\sin\theta)\tilde{d}_\downarrow]$, $d_R = e^{-i\phi_R}[(\sin\theta)\tilde{d}_\uparrow + (\cos\theta)\tilde{d}_\downarrow]$, $c_{\mathbf{k}L} = e^{-i\phi_L}[(\cos\theta)\tilde{c}_{\mathbf{k}\uparrow} - (\sin\theta)\tilde{c}_{\mathbf{k}\downarrow}]$ and $c_{\mathbf{k}R} = e^{-i\phi_R}[(\sin\theta)\tilde{c}_{\mathbf{k}\uparrow} + (\cos\theta)\tilde{c}_{\mathbf{k}\downarrow}]$ into the Hamiltonian of Eq.(1), in particular at the zero-bias regime ($\mu_\alpha = 0 \equiv$Fermi level of the leads), we obtain

$$\mathcal{H}_{\text{Full}} = \sum_{\mathbf{k},\sigma} \tilde{\varepsilon}_{\mathbf{k}} \tilde{c}^\dagger_{\mathbf{k}\sigma} \tilde{c}_{\mathbf{k}\sigma} + \sum_\sigma \epsilon_{d\sigma} \tilde{d}^\dagger_\sigma \tilde{d}_\sigma + \mathcal{V}\sum_{\mathbf{k},\sigma}(\tilde{c}^\dagger_{\mathbf{k}\sigma} \tilde{d}_\sigma + \text{H.c.})$$
$$+ \mathcal{H}_{\text{MFs}}, \tag{3}$$

which mimics an effective single QD coupled to an unique lead both exhibiting an artificial spin degree of freedom $\sigma = \pm 1$ ($\uparrow,\downarrow$) (see Fig. 1(c) for such a representation).

We call attention that from now on, we label the aforementioned variable by *pseudospin*. As in Ref.[33], we have topological protection of our findings if the phase difference $\phi_L - \phi_R = 2n\pi$ is fulfilled, with n integer being tunable via magnetic flux, thus leading to $\cos(2\theta) = \frac{\triangle\epsilon \cos(\phi_L - \phi_R)}{\sqrt{4(T_c)^2 + (\triangle\epsilon)^2}}$, $\triangle\epsilon = \varepsilon_L - \varepsilon_R$ as the detuning of the original spinless QDs, the *pseudo*-Zeeman gap $\epsilon_{d\uparrow} - \epsilon_{d\downarrow}$, with $\epsilon_{d\sigma} = \frac{(\varepsilon_L + \varepsilon_R)}{2} + \frac{\sigma}{2}\sqrt{4(T_c)^2 + (\triangle\epsilon)^2}$ and

$$\mathcal{H}_{\text{MFs}} = \varepsilon_M(\eta^\dagger_\uparrow \eta_\uparrow - \frac{1}{2}) + \sum_\sigma \bar{\lambda}_\sigma(\tilde{d}_\sigma \eta^\dagger_\uparrow + \tilde{d}_\sigma \eta_\uparrow + \text{H.c.}), \tag{4}$$

where we have used $\Psi_1 = \frac{1}{\sqrt{2}}\left(\eta^\dagger_\uparrow + \eta_\uparrow\right)$ and $\Psi_2 = \frac{i}{\sqrt{2}}\left(\eta^\dagger_\uparrow - \eta_\uparrow\right)$ in order to build the *qubit* $\eta_\uparrow$ composed by the MFs, namely the MF-*qubit*, with $\bar{\lambda}_\uparrow = \frac{1}{\sqrt{2}}(|\lambda_L|\cos\theta + |\lambda_R|\sin\theta)$ and $\bar{\lambda}_\downarrow = \frac{1}{\sqrt{2}}(|\lambda_R|\cos\theta - |\lambda_L|\sin\theta)$ as *pseudospin*-dependent amplitudes. As a result, the *pseudo*-Zeeman gap becomes dressed by such an interaction, i.e., $\tilde{\epsilon}_{d\uparrow} - \tilde{\epsilon}_{d\downarrow}$, which will be addressed later on.

We call attention to the system Hamiltonian mapping into Eq.(4), where one can recognize that the device of Fig. 1(b) is equivalent to the QD $\tilde{d}_\sigma$ emulating the two original spinless left and right QDs, in particular sidecoupled to $\eta_\uparrow$, which corresponds to a QD replacing the Kitaev chain. This opens the possibility of reproducing experimentally the same phenomenon reported here for the topological Kitaev chain by employing QDs, but in the presence of a delocalized Cooper pair split into $\tilde{d}_\sigma$ and $\eta_\uparrow$ with pairing amplitude $\bar{\lambda}_\sigma$ as the terms $\bar{\lambda}_\sigma(\tilde{d}_\sigma\eta_\uparrow + \text{H.c.})$ point out. Besides, the normal tunneling between these QDs should be also equal to $\bar{\lambda}_\sigma$, i.e., $\bar{\lambda}_\sigma(\tilde{d}_\sigma\eta^\dagger_\uparrow + \text{H.c.})$, just in order to ensure the emergence of MFs at the so-called "sweet spot" as predicted in Ref.[36] by Flensberg. In such a work, the equivalence of the topological Kitaev chain with a QD system is established by means of an analogous Hamiltonian to our Eq.(4). In this way, this system of QDs hosting MFs becomes an experimental alternative with respect to the topological Kitaev chain. Noteworthy, this QD-like alternative system with MFs was already explored by some of us in Ref.[37] within

the context of adatoms and STM tips as well as the case of a zero-mode from a regular normal side-coupled QD to a central QD region[38]. For this latter, the *qubit* $\eta_\uparrow$ without the Cooper pairing amplitude (proximity effect) when encrypted would be still protected against the decoherence of the surroundings due to the BIC nature of the state which decouples it from the environment, thus preventing a finite conductance through this channel. Equivalently, BICs do not depend on the proximity effect to occur. However, the decrypted *qubit* case would not be protected in the same way, once it couples to the environment in contrast to a MF-*qubit*, which is topologically protected characterized by a pinned ZBP. This characteristic plays the main difference from a regular fermionic zero-mode, wherein the expected ZBP is destroyed by changing external parameters as outlined in Fig.4(a) of Ref.[38] and the readout of the *qubit* in the central QD region is compromised as a result.

In what follows, we use the Landauer-Büttiker formula for the zero-bias conductance $\mathcal{G}$[39] to analyze the transport through the QDs, which is

$$\mathcal{G} = \frac{e^2}{h} \int d\varepsilon \left(-\frac{\partial f_F}{\partial \varepsilon} \right) \mathcal{T}_{\text{Total}}, \qquad (5)$$

where f_F stands for the Fermi-Dirac distribution, $\mathcal{T}_{\text{Total}} = \sum_j \mathcal{T}_{jj} + \sum_j \mathcal{T}_{j\bar{j}}$ encodes the system total transmittance with $j = L, R$ respectively for $\bar{j} = R, L$ to correlate distinct QDs, in which $\mathcal{T}_{jl} = \mathcal{T}_{\uparrow\uparrow} + \mathcal{T}_{\downarrow\downarrow} + \mathcal{T}_{\uparrow\downarrow} + \mathcal{T}_{\downarrow\uparrow}$ dictates the transmittance through the channels $l, j = L, R$ in terms of the coefficients $\mathcal{T}_{\sigma\bar{\sigma}}$ for the *pseudospin* representation.

Furthermore, $\mathcal{T}_{jl} = \pi\Gamma \rho_{jl}$ depends upon the Anderson broadening $\Gamma = \pi\mathcal{V}^2 \sum_\mathbf{k} \delta(\varepsilon - \tilde{\varepsilon}_\mathbf{k})$ [40] and $\rho_{jl} = (-1/\pi)\text{Im}(\tilde{\mathcal{G}}_{d_j,d_l})$, the densities of states for the spinless QDs from the Hamiltonian of Eq.(1) in terms of the retarded Green's functions $\tilde{\mathcal{G}}_{d_j,d_l}$, which are given by

$$\rho_{LL} = -\frac{1}{\pi}\text{Im}\{\cos^2\theta \tilde{\mathcal{G}}_{\tilde{d}_\uparrow,\tilde{d}_\uparrow} + \sin^2\theta \tilde{\mathcal{G}}_{\tilde{d}_\downarrow,\tilde{d}_\downarrow} - \sin\theta\cos\theta(\tilde{\mathcal{G}}_{\tilde{d}_\downarrow,\tilde{d}_\uparrow} + \tilde{\mathcal{G}}_{\tilde{d}_\uparrow,\tilde{d}_\downarrow})\}, \qquad (6)$$

$$\rho_{RR} = -\frac{1}{\pi}\text{Im}\{\sin^2\theta \tilde{\mathcal{G}}_{\tilde{d}_\uparrow,\tilde{d}_\uparrow} + \cos^2\theta \tilde{\mathcal{G}}_{\tilde{d}_\downarrow,\tilde{d}_\downarrow} + \sin\theta\cos\theta(\tilde{\mathcal{G}}_{\tilde{d}_\downarrow,\tilde{d}_\uparrow} + \tilde{\mathcal{G}}_{\tilde{d}_\uparrow,\tilde{d}_\downarrow})\}, \qquad (7)$$

$$\rho_{RL} = -\frac{1}{\pi}\text{Im}\{\sin\theta\cos\theta(\tilde{\mathcal{G}}_{\tilde{d}_\uparrow,\tilde{d}_\uparrow} - \tilde{\mathcal{G}}_{\tilde{d}_\downarrow,\tilde{d}_\downarrow}) + \cos^2\theta \tilde{\mathcal{G}}_{\tilde{d}_\downarrow,\tilde{d}_\uparrow} - \sin^2\theta \tilde{\mathcal{G}}_{\tilde{d}_\uparrow,\tilde{d}_\downarrow}\} \qquad (8)$$

and

$$\rho_{LR} = -\frac{1}{\pi}\text{Im}\{\sin\theta\cos\theta(\tilde{\mathcal{G}}_{\tilde{d}_\uparrow,\tilde{d}_\uparrow} - \tilde{\mathcal{G}}_{\tilde{d}_\downarrow,\tilde{d}_\downarrow}) - \sin^2\theta \tilde{\mathcal{G}}_{\tilde{d}_\downarrow,\tilde{d}_\uparrow} + \cos^2\theta \tilde{\mathcal{G}}_{\tilde{d}_\uparrow,\tilde{d}_\downarrow}\}, \qquad (9)$$

here written as functions of the retarded Green's functions $\tilde{\mathcal{G}}_{\tilde{d}_\sigma,\tilde{d}_{\tilde{\sigma}}}$ within the mapping on the *pseudospin* degree. To evaluate $\tilde{\mathcal{G}}_{\tilde{d}_\sigma,\tilde{d}_{\tilde{\sigma}}}$, we should employ the equation-of-motion method[39] by using Eqs.(3) and (4) as follows: $\varepsilon\tilde{\mathcal{G}}_{\tilde{d}_\sigma,\tilde{d}_{\tilde{\sigma}}} = [\tilde{d}_\sigma, \tilde{d}_{\tilde{\sigma}}^\dagger]_+ + \tilde{\mathcal{G}}_{[\tilde{d}_\sigma,\mathcal{H}_{\text{Full}}],\tilde{d}_{\tilde{\sigma}}}$. As a result, we find the linear system:

$$(\varepsilon - \epsilon_{d\sigma} - \bar{\lambda}_\sigma^2 K + i\Gamma)\tilde{\mathcal{G}}_{\tilde{d}_\sigma,\tilde{d}_{\tilde{\sigma}}} - \bar{\lambda}_{\bar{\sigma}}\bar{\lambda}_\sigma K\tilde{\mathcal{G}}_{\tilde{d}_{\bar{\sigma}},\tilde{d}_{\tilde{\sigma}}}$$
$$+\bar{\lambda}_\sigma^2 K\tilde{\mathcal{G}}_{\tilde{d}_\sigma^\dagger,\tilde{d}_{\tilde{\sigma}}} + \bar{\lambda}_\sigma\bar{\lambda}_{\bar{\sigma}} K\tilde{\mathcal{G}}_{\tilde{d}_{\bar{\sigma}}^\dagger,\tilde{d}_{\tilde{\sigma}}} = 1, \qquad (10)$$

$$-\bar{\lambda}_\sigma\bar{\lambda}_{\bar{\sigma}} K\tilde{\mathcal{G}}_{\tilde{d}_\sigma,\tilde{d}_{\tilde{\sigma}}} + (\varepsilon - \epsilon_{d\sigma} - \bar{\lambda}_\sigma^2 K + i\Gamma)\tilde{\mathcal{G}}_{\tilde{d}_\sigma,\tilde{d}_{\tilde{\sigma}}}$$
$$+\bar{\lambda}_\sigma\bar{\lambda}_{\bar{\sigma}} K\tilde{\mathcal{G}}_{\tilde{d}_{\bar{\sigma}}^\dagger,\tilde{d}_{\tilde{\sigma}}} + \bar{\lambda}_\sigma^2 K\tilde{\mathcal{G}}_{\tilde{d}_\sigma^\dagger,\tilde{d}_{\tilde{\sigma}}} = 0, \qquad (11)$$

$$\bar{\lambda}_\sigma^2 K\tilde{\mathcal{G}}_{\tilde{d}_\sigma,\tilde{d}_{\tilde{\sigma}}} + \bar{\lambda}_\sigma\bar{\lambda}_{\bar{\sigma}} K\tilde{\mathcal{G}}_{\tilde{d}_{\bar{\sigma}},\tilde{d}_{\tilde{\sigma}}}$$
$$+(\varepsilon + \epsilon_{d\sigma} - \bar{\lambda}_\sigma^2 K + i\Gamma)\tilde{\mathcal{G}}_{\tilde{d}_\sigma^\dagger,\tilde{d}_{\tilde{\sigma}}} - \bar{\lambda}_\sigma\bar{\lambda}_{\bar{\sigma}} K\tilde{\mathcal{G}}_{\tilde{d}_{\bar{\sigma}}^\dagger,\tilde{d}_{\tilde{\sigma}}} = 0 \qquad (12)$$

and

$$\bar{\lambda}_\sigma\bar{\lambda}_{\bar{\sigma}} K\tilde{\mathcal{G}}_{\tilde{d}_\sigma,\tilde{d}_{\tilde{\sigma}}} + \bar{\lambda}_\sigma^2 K\tilde{\mathcal{G}}_{\tilde{d}_\sigma,\tilde{d}_{\tilde{\sigma}}} - \bar{\lambda}_{\bar{\sigma}}\bar{\lambda}_\sigma K\widetilde{\mathcal{G}}_{\tilde{d}_{\bar{\sigma}}^\dagger,\tilde{d}_{\tilde{\sigma}}}$$
$$+(\varepsilon + \epsilon_{d\sigma} - \bar{\lambda}_\sigma^2 K + i\Gamma)\tilde{\mathcal{G}}_{\tilde{d}_\sigma^\dagger,\tilde{d}_{\tilde{\sigma}}} = 0, \qquad (13)$$

where $\bar{\sigma}$ is the opposite of σ and $K = (\varepsilon + \varepsilon_M)^{-1} + (\varepsilon - \varepsilon_M)^{-1}$. To perform the analysis of the model in the next section, we make explicit that we have solved the current system numerically.

Results and Discussion.—In the simulations below the temperature $T = 0$ is assumed and $\Gamma = 40\mu eV$[8, 40] as the energy scale. The topological Kitaev chain, for a sake of simplicity, is treated as very large, which imposes $\varepsilon_M \to 0$. Thus, in order to make explicit the phenomenon of MF-*qubit* cryptography, we begin discussing the picture requested for the emergence of such in Fig.2. Fig.2(a) accounts for $\varepsilon_R = -2\Gamma$, $|\lambda_L| = |\lambda_R| = \lambda = 5\Gamma$, $T_c = 1\Gamma$ and $\varepsilon_L = 1\Gamma$, where we verify a ZBP with amplitude of $1/4$ in $\mathcal{T}_{\text{Total}}$ of Eq.(5) as a function of ε. This detectable resonance represents the leakage of the MF-*qubit* $\eta_\uparrow$ into the double QD setup. Additionally, it also encodes the recording of a decrypted MF-*qubit* over the left QD, which will be elucidated later on via Figs.3 and 4. On this ground, let us consider the sequence of panels from (b) to (d), which describes the *qubit* cryptography itself: by changing just ε_L, we notice that the ZBP amplitude becomes reduced progressively up to entire quenching in Fig.2(d). In this case, solely a couple of peaks stay visible denoting the dressed *pseudo*-Zeeman gap $\tilde{\epsilon}_{d\uparrow} - \tilde{\epsilon}_{d\downarrow}$. Indeed, we will clarify that the ZBP becomes BICs, being undetectable by $\mathcal{T}_{\text{Total}}$. It means that if the ZBP is not perceived, we have the accomplishment of the MF-*qubit* cryptography, which appears addressed in detail by Figs.3 and 4.

Fig.3 exhibits the density plots for $\mathcal{T}_{\text{Total}}, \mathcal{T}_{LL}$ and $\mathcal{T}_{RR}$ spanned by the axis ε and ε_L for fixed $\varepsilon_R = -2\Gamma$ ($\varepsilon_R = -1.5\Gamma$) $\lambda = 5\Gamma$ ($|\lambda_L| = 1.95\Gamma$ and $|\lambda_R| = 5\Gamma$) and
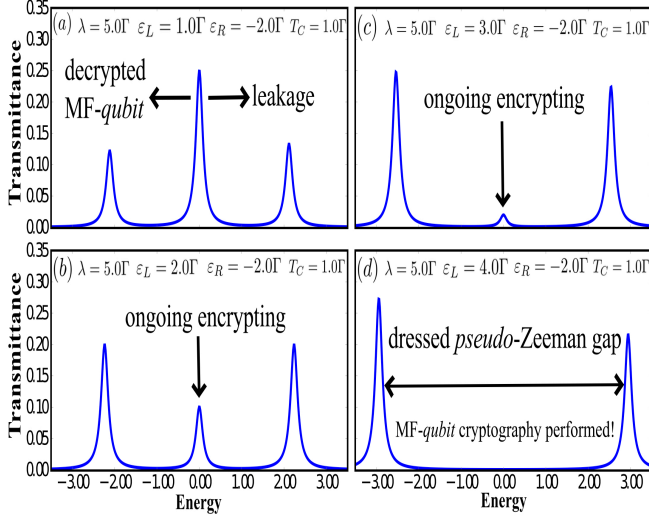
Figure 2. (Color online) $\mathcal{T}_{\text{Total}}$ as a function of ε: (a) The ZBP gives the asymmetrical leakage of the MF-*qubit* $\eta_\uparrow$ into the left QD (see also Fig.3). (b)-(c) The increasing of ε_R yields the process for encrypting this *qubit*, which is characterized by the quenching of the ZBP amplitude. (d) Here the ZBP (the MF-*qubit*) is hidden as BICs equally split into the QDs, where only the dressed *pseudo*-Zeeman gap is visible (see also Fig.4).

$T_c = 1\Gamma$. It is worth noticing that all panels in Figs.3(a)-(f) present a ZBP structure. However, each one reveals different aspects on the leakage effect. For instance, in Fig.3(a)((d)) we highlight the upper region marked by a yellow dashed ellipse: it gives the domain where the MF-*qubit* cryptography is allowed, once the ZBP is absent. Figs.3(b)((e)) and (c)((f)) contain the asymmetrical leakage into the QDs and the decrypted MF-*qubit* left recording as well. Notice that in the latter, nearby $\varepsilon_L = 1\Gamma$ ($\varepsilon_L = 0$), the right QD decouples from the setup, due to $\mathcal{T}_{RR} = 0$. This region is then identified by white dashed ellipses in panels (a)-(f) of the same figure. As a result, the MF state is recorded solely at the left QD as Fig.3(b)((e)) ensures. This corresponds to the readout of the *qubit* by a charge measurement as proposed by Flensberg[33]. Notice that both $\mathcal{T}_{LL}$ and $\mathcal{T}_{RR}$ share the same brightness in their scales, thus pointing out the symmetrical leakage of the MF zero-mode is robust against asymmetrical couplings. Concerning the satellite arcs aside the ZBP in Figs.3(a)-(f), they account for the dressed *pseudo*-Zeeman gap $\tilde{\epsilon}_{d\uparrow} - \tilde{\epsilon}_{d\downarrow}$. These arcs are predominantly absent, as we can see, at the lower region of Fig.3(a). This points out that BICs away from the ZB limit are also reliable in this device. Thereby, in order to fully understand the underlying physics on the decrypted MF-*qubit* left recording versus the MF-*qubit* cryptography, we should consider Fig.4, which uses the same parameters of Fig.2 just for a matter of choice, once for the emergence of the BICs the leakage is always symmetrical even with asymmetrical couplings λ_L and λ_R as
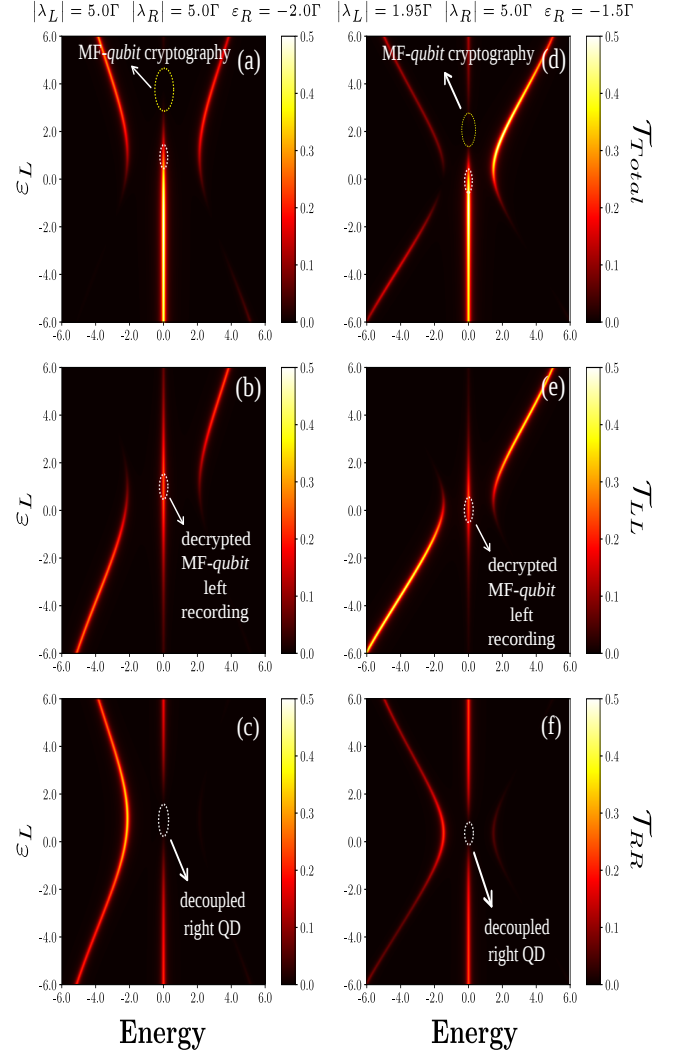

Figure 3. (Color online) Density plots of: (a) $\mathcal{T}_{\text{Total}}$, (b) $\mathcal{T}_{LL}$ and (c) $\mathcal{T}_{RR}$ spanned by ε_L and ε, with $\varepsilon_R = -2\Gamma$, $|\lambda_L| = |\lambda_R| = \lambda = 5\Gamma$ and $T_c = 1\Gamma$. The ellipses depicted show at zero-bias: i) the region for the MF-*qubit* cryptography (yellow dashed ellipse) in (a) and ii) the corresponding for the decrypted MF-*qubit* left recording (white dashed ellipse) in (a) and (b), due to the right QD entirely decoupled from the system as panel (c) shows (white dashed ellipse). Panels (d),(e) and (f) for $|\lambda_L| \neq |\lambda_R|$ give qualitatively the same of (a),(b) and (c) thus ensuring the topological robustness of the results, i.e., the BICs (the encrypted MF-*qubit*) and the decrypted MF-*qubit* left recording still occur, but for different set of parameters.

Figs.3(e) and (f) ensure.

In Fig.4(a) the analysis of $\mathcal{T}_{jl}$ shows that the leakage of the MF occurs only over the left QD. In this way, the decrypted MF-*qubit* situation is achieved: $\mathcal{T}_{LL}$ exhibits a ZBP with amplitude $1/4$ in contrast to $\mathcal{T}_{RR}$. Thus in order to understand such an issue, we should focus on the insets. $\mathcal{T}_{RR}$ presents $\mathcal{T}_{\uparrow\uparrow}+\mathcal{T}_{\downarrow\downarrow}$ perfectly phase shifted by π with respect to $\mathcal{T}_{\uparrow\downarrow}+\mathcal{T}_{\downarrow\uparrow}$(Fano dip)[41, 42], thus resulting
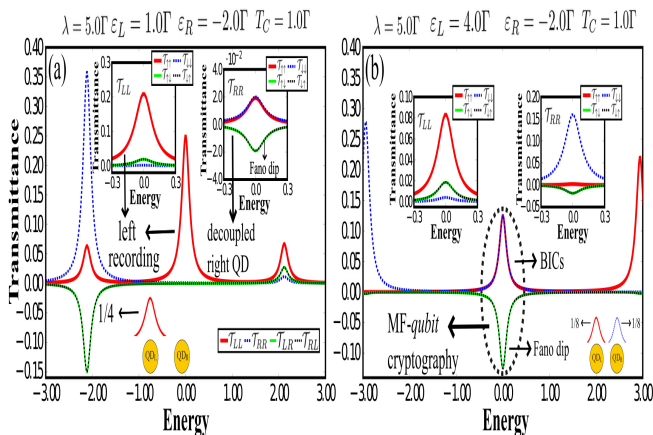
Figure 4. (Color online) $\mathcal{T}_{jl}$ in (a) characterizing the de-crypted MF-*qubit* left recording. $\mathcal{T}_{LL}$ shows a ZBP with amplitude 1/4, while $\mathcal{T}_{RR}$ does not: the inset reveals that $\mathcal{T}_{RR}$ exhibits $\mathcal{T}_{\uparrow\uparrow} + \mathcal{T}_{\downarrow\downarrow}$ perfectly phase shifted by π with respect to $\mathcal{T}_{\uparrow\downarrow} + \mathcal{T}_{\downarrow\uparrow}$ (Fano dip). As aftermath, this QD is disconnected from the system. In (b), we have the MF-*qubit* cryptography: in $\mathcal{T}_{RR}$, the Fano dip is not perfect as before. However, a Fano dip in $\mathcal{T}_{LR} + \mathcal{T}_{RL}$ interferes destructively and exactly with $\mathcal{T}_{LL} + \mathcal{T}_{RR}$. It means that MF-*qubit* is hidden as BICs equally divided into the QDs.

in a decoupled QD from the setup. For $\mathcal{T}_{LL}$, $\mathcal{T}_{\uparrow\uparrow} + \mathcal{T}_{\downarrow\downarrow}$ and $\mathcal{T}_{\uparrow\downarrow} + \mathcal{T}_{\downarrow\uparrow}$ interfere constructively. In Fig.4(b) for $\mathcal{T}_{RR}$, the Fano dip in $\mathcal{T}_{\uparrow\downarrow} + \mathcal{T}_{\downarrow\uparrow}$ is not perfect as previously and does not cancel $\mathcal{T}_{\uparrow\uparrow} + \mathcal{T}_{\downarrow\downarrow}$ anymore. Particularly, the Fano dip found in $\mathcal{T}_{LR} + \mathcal{T}_{RL}$ interferes destructively and perfectly with the peak in $\mathcal{T}_{LL} + \mathcal{T}_{RR}$. Finally, this yields the MF-*qubit* cryptography here proposed. In this way,

the recording of the *qubit* is found secure at two apart sites and hidden as BICs, which are equally split into the QDs and with amplitude 1/8 each. These processes appear outlined in the sketches placed at the lower region of Figs.4(a) and (b).

Interestingly enough, the underlying physics of this cryptography assisted by BICs has a simple picture: the electronic waves traveling forth and back between the QDs ($\mathcal{T}_{LR} + \mathcal{T}_{RL}$), in particular at zero-bias, interfere destructively with those waves that only pass through these QDs ($\mathcal{T}_{LL} + \mathcal{T}_{RR}$) and as a result, the BICs within the latter emerge. Regarding the satellite arcs aside the ZBP in Figs.4(a) and (b), we should mention that they are also the result of interference processes in $\mathcal{T}_{jl}$ as observed.

Conclusions.—In summary, we have found theoretically that the cryptography of the MF-*qubit* is feasible in the system of Fig.1(a). We have showed that the recording of the MF-*qubit* over a single QD is due to an asymmetrical leakage of the MF state into the QDs. The encrypted MF-*qubit* is performed when the leaking is symmetrical, wherein the MF-leaked state becomes BICs. Thus we reveal a switch on/off mechanism for the read-out of the *qubit* $\eta_{\uparrow} = \frac{1}{\sqrt{2}} (\Psi_1 + i\Psi_2)$ by means of its ZBP fingerprint on the QDs, which provides a way of performing quantum cryptography regarding the message written inside the MFs states Ψ_1 and Ψ_2 initially prepared at the edges of a topological Kitaev chain. Therefore, we trust that our findings can be applied to quantum processing issues in topological quantum computation devices.

[1] J. Alicea, Rep. Prog. Phys. **75**, 076501 (2012).
[2] S. R. Elliott and M. Franz, Rev. Mod. Phys. **87**, 137 (2015).
[3] A. Y. Kitaev, Phys. Usp. **44**, 131 (2001).
[4] A. A. Zyuzin, D. Rainis, J. Klinovaja, and D. Loss, Phys. Rev. Lett. **111**, 056802 (2013).
[5] D. Rainis, J. Klinovaja, L. Trifunovic, and D. Loss, Phys. Rev. B **87**, 024515 (2013).
[6] A. Zazunov, P. Sodano, and R. Egger, New J. Phys **15**, 035033 (2013).
[7] D. Roy, C. J. Bolech, and N. Shah, Phys. Rev. B **86**, 094503 (2012).
[8] E. Vernek, P. H. Penteado, A. C. Seridonio, and J. C. Egues, Phys. Rev. B **89**, 165314 (2014).
[9] M. T. Deng, S. Vaitiekenas, E. B. Hansen, J. Danon, M. Leijnse, K. Flensberg, J. Nygard, P. Krogstrup, and C. M. Marcus, Science **354**, 6319 (2016).
[10] G. Moore and N. Read, Nucl. Phys. B **360**, 362 (1991).
[11] L. Fu, C. L. Kane, and E. J. Mele, Phys. Rev. Lett. **98**, 106803 (2007).
[12] L. Fu and C.L. Kane, Phys. Rev. Lett. **100**, 096407 (2008).
[13] J. D. Sau, R. M. Lutchyn, S. Tewari, and S. Das Sarma, Phys. Rev. Lett. **104**, 040502 (2010).
[14] T. Kawakami and X. Hu, Phys. Rev. Lett. **115**, 177001 (2015).
[15] S. N.- Perge, I. K. Drozdov, J. Li, H. Chen, S. Jeon, J. Seo, A. H. MacDonald, B. A. Bernevig, and A. Yazdani, Science **346**, 602 (2014).
[16] R. Pawlak, M. Kisiel, J. Klinovaja, T. Meier, S. Kawai, T. Glatzel, D. Loss, and E. Meyer, Nature Partner Journals Quantum Information **2**, 16035 (2016).
[17] V. Mourik, K. Zuo, S. M. Frolov, S. R. Plissard, E. P. A. M. Bakkers, and L. P. Kouwenhoven, Science **336**, 1003 (2012).
[18] J. von Neumann and E. Wigner, Phys. Z. **30**, 465 (1929).
[19] F. H. Stillinger and D. R. Herrick, Phys. Rev. A **11**, 446 (1975).
[20] C. W. Hsu, B. Zhen, A. D. Stone, J. D. Joannopoulos, and M. Soljacic, Nature Review Materials, **1**, 16048 (2016).
[21] L. H. Guessi, Y. Marques, R. S. Machado, L.S. Ricco, K. Kristinsson, M. S. Figueira, I. A. Shelykh, M. de Souza, and A. C. Seridonio, Phys. Rev. B **92**, 245107 (2015).

[22] L. H. Guessi, R. S. Machado, Y. Marques, L. S. Ricco, K. Kristinsson, M. Yoshida, I.A. Shelykh, M. de Souza, and A. C. Seridonio, Phys. Rev. B **92**, 045409 (2015).

[23] W.-J. Gong, X.-Y. Sui, Y. Wang, G.-D. Yu, and X.-H. Chen, Nanoscale Research Letters 8, 330 (2013).

[24] Y. Boretz, G. Ordonez, S. Tanaka, and T. Petrosky, Phys. Rev. A **90**, 023853 (2014)

[25] A. Crespi, L. Sansoni, G. D. Valle, A. Ciamei, R. Ramponi, F. Sciarrino, P. Mataloni, S. Longhi, and R. Osellame, Phys. Rev. Lett. **114**, 090201 (2015).

[26] C. W. Hsu, B. Zhen, J. Lee, S.-L. Chua, S. G. Johnson, J.D. Joannopoulos, and M. Soljačić, Nature **499**, 188 (2013).

[27] Y. Plotnik, O. Peleg, F. Dreisow, M. Heinrich, S. Nolte, A. Szameit, and M. Segev, Phys. Rev. Lett. **107**, 183901 (2011).

[28] J. M.-Petit and R. A. Molina, Phys. Rev. B **90**, 035434 (2014).

[29] G. D. Valle and S. Longhi, Phys. Rev. B **89**, 115118 (2014).

[30] C. González-Santander, P. A. Orellana, and F. Domínguez-Adame, Europhys. Lett. **102**, 17012 (2013).

[31] L. S. Ricco, Y. Marques, F. A. Dessotti, R. S. Machado, M. de Souza, and A. C. Seridonio Phys. Rev. B **93**, 165116 (2016).

[32] F. A. Dessotti, L. S. Ricco, Y. Marques, L. H. Guessi, M. Yoshida, M. S. Figueira, M. de Souza, Pasquale Sodano, and A. C. Seridonio Phys. Rev. B **94**, 125426 (2016).

[33] Karsten Flensberg, Phys. Rev. Lett. **106**, 090503 (2011).

[34] D. E. Liu and H. U. Baranger, Phys. Rev. B **84**, 201308(R) (2011).

[35] M. Leijnse and K. Flensberg, Phys. Rev. B **84**, 140501(R) (2011).

[36] M. Leijnse and K. Flensberg, Phys. Rev. B **86**, 134528 (2012).

[37] F.A. Dessotti, L.S. Ricco, Y. Marques, R.S. Machado, L.H. Guessi, M.S. Figueira, M. de Souza, and A.C. Seridonio, Physica E **83**, 297 (2016).

[38] F.A. Dessotti, L.S. Ricco, M. de Souza, F.M. Souza, and A.C. Seridonio, J. Appl. Phys. **116**, 173701 (2014).

[39] H. Haug and A. P. Jauho, Quantum Kinetics in Transport and Optics of Semiconductors, Springer Series in Solid-State Sciences 123 (Springer, New York, 1996).

[40] P. W. Anderson, Phys. Rev. **124**, 41 (1961).

[41] U. Fano, Phys. Rev. **124**, 1866 (1961). r d

[42] A. E. Miroshnichenko, S. Flach, and Y. S. Kivshar, Rev. Mod. Phys. **82**, 2257 (2010).